Empire XPU Code Verification Report for IEC/IEEE 62704-1

EMPIRE XPU Version 9.0.1
03.07.2024, Build 22948

Contents

1 Introduction

This report demonstrates the compliance of the EMPIRE XPU software version 9.0.1 with code verification requirements defined in IEC/IEEE 62704-1 standard. The compliance of EMPIRE XPU software with IEC/IEEE 62704-1 code verification requirements makes it applicable for determining the peak spatial-average Specific Absorption Rate (SAR) in the human body from wireless devices , for mobile devices held in proximity with the human head or body, as well as for exposure to the field radiated by vehicle-mounted antenna, as respectively described in IEC/IEEE 62704-2 and IEC/IEEE 62704-3 international standards. The IEC/IEEE 62704-4 concerns the Finite Element Method (FEM) and does therefore not apply to Empire XPU.

1.1 Normative References

Normative References			
	Test Standard	Description	Issue Date
☒	IEC/IEEE 62704-1	Determining the peak spatial-average specific absorption rate (SAR) in the human body from wireless communications devices, 30 MHz to 6 GHz - Part 1: General requirements for using the finite difference time-domain (FDTD) method for SAR calculations	October 26, 2017
☒	IEC/IEEE 62704-2	Determining the peak spatial-average specific absorption rate (SAR) in the human body from wireless communications devices, 30 MHz to 6 GHz - Part 2: Specific requirements for finite difference time domain (FDTD) modelling of exposure from vehicle mounted antennas	June 28, 2017
☒	IEC/IEEE 62704-3	Determining the peak spatial-average specific absorption rate (SAR) in the human body from wireless communications devices, 30 MHz to 6 GHz - Part 3: Specific requirements for using the finite difference time domain (FDTD) method for SAR calculations of mobile phones	October 26, 2017
☐	IEC/IEEE 62704-4	Determining the peak spatial-average specific absorption rate (SAR) in the human body from wireless communication devices, 30 MHz to 6 GHz - Part 4: General requirements for using the finite element method for SAR calculations	October 20, 2020

Table 1: Normative references

1.2 Attestation of Verification Results

All required verification results calculated with Empire XPU are within the tolerances allowed by the IEC/IEEE 62704-1, as demonstrated in detail in the following sections of this report (all tests passed). Therefore it can be stated, that Empire XPU is compliant with the standards code verification requirements.

1.3 Quality Assurance

The responsible engineer states that all code verification tests have been performed under the guidelines of the IEC/IEEE 62704-1.

Prepared by:	A. Wien	Reviewed by:	W. Simon
	Andreas Wien Engineer		Winfried Simon Team Leader EM-Modeling

2 Code Accuracy

2.1 Free Space Characteristics

The simulation model has been set up as defined in section 8.2.1 of IEC/IEEE 62704-1. This section shows the maximum deviation of the wave numbers from the reference

Numerical Dispersion Characteristics for $+X$ Axis and Y Orientation of the Electric Field							
	Limit for code compliance	**TE**			**TM**		
ε_r		1	2	2	1	2	2
σ [S/m]		0	0	0.2	0	0	0.2
numerical f_{cutoff} [MHz]		1247	882	<500	1247	882	<500
max. dev. of simulated Re$\{k_z\}$ from numerical reference homogeneous mesh	$\pm$2 %	1.07 %	1.3 %	0.78 %	1.08 %	-0.29 %	0.41 %
max. dev. of simulated Im$\{k_z\}$ from numerical reference homogeneous mesh	$\pm$2 %	n.a.	n.a.	1.24 %	n.a.	n.a.	1.14 %
max. dev. of simulated Re$\{k_x\}$ from numerical reference homogeneous mesh	$\pm$2 %	1.16 %	-0.51 %	<0.01 %	-0.76 %	-0.75 %	<0.01 %
max. dev. of simulated Re$\{k_z\}$ from physical solution inhomogeneous mesh	$\pm$10 %	-4.69 %	4.02 %	0.93 %	4.65 %	4.29 %	-0.46 %
max. dev. of simulated Im$\{k_z\}$ from physical solution inhomogeneous mesh	$\pm$10 %	n.a.	n.a.	2.69 %	n.a.	n.a.	0.78 %
max. dev. of simulated Re$\{k_x\}$ from physical solution inhomogeneous mesh	$\pm$10 %	-2.6 %	1.48 %	5.55 %	0.41 %	0.99 %	0.64 %
NOTE 1 The frequency range $\pm$5 % around the cutoff frequencies can be excluded from the evaluation of the k_z components.							

Table 2: Results of the evaluation of the numerical dispersion characteristics for +x axis and y orientation of the electric field.

Numerical Dispersion Characteristics for $+$X Axis and Z Orientation of the Electric Field							
	Limit for code compliance	**TE**			**TM**		
ε_r		1	2	2	1	2	2
σ [S/m]		0	0	0.2	0	0	0.2
numerical f_{cutoff} [MHz]		1247	882	<500	1247	882	<500
max. dev. of simulated Re$\{k_z\}$ from numerical reference homogeneous mesh	$\pm$2 %	1.14 %	0.8 %	0.41 %	1.1 %	0.86 %	0.78 %
max. dev. of simulated Im$\{k_z\}$ from numerical reference homogeneous mesh	$\pm$2 %	n.a.	n.a.	1.14 %	n.a.	n.a.	1.24 %
max. dev. of simulated Re$\{k_x\}$ from numerical reference homogeneous mesh	$\pm$2 %	-1.36 %	-1.15 %	<0.01 %	0.38 %	1.68 %	<0.01 %
max. dev. of simulated Re$\{k_z\}$ from physical solution inhomogeneous mesh	$\pm$10 %	-4.68 %	-6.61 %	0.92 %	4.65 %	4.29 %	-0.46 %
max. dev. of simulated Im$\{k_z\}$ from physical solution inhomogeneous mesh	$\pm$10 %	n.a.	n.a.	2.69 %	n.a.	n.a.	0.78 %
max. dev. of simulated Re$\{k_x\}$ from physical solution inhomogeneous mesh	$\pm$10 %	7.39 %	0.39 %	5.55 %	0.44 %	0.56 %	0.64 %
NOTE 1 The frequency range $\pm$5 % around the cutoff frequencies can be excluded from the evaluation of the k_z components.							

Table 3: Results of the evaluation of the numerical dispersion characteristics for +x axis and z orientation of the electric field.

Numerical Dispersion Characteristics for $+$Y Axis and X Orientation of the Electric Field							
	Limit for code compliance	**TE**			**TM**		
ε_r		1	2	2	1	2	2
σ [S/m]		0	0	0.2	0	0	0.2
numerical f_{cutoff} [MHz]		1247	882	<500	1247	882	<500
max. dev. of simulated Re$\{k_z\}$ from numerical reference homogeneous mesh	$\pm$2 %	1.04 %	1.3 %	0.78 %	1.08 %	-0.3 %	0.41 %
max. dev. of simulated Im$\{k_z\}$ from numerical reference homogeneous mesh	$\pm$2 %	n.a.	n.a.	1.24 %	n.a.	n.a.	1.14 %
max. dev. of simulated Re$\{k_x\}$ from numerical reference homogeneous mesh	$\pm$2 %	-0.54 %	0.04 %	<0.01 %	0.49 %	1.26 %	<0.01 %
max. dev. of simulated Re$\{k_z\}$ from physical solution inhomogeneous mesh	$\pm$10 %	-4.69 %	4.02 %	0.93 %	4.65 %	4.29 %	-0.46 %
max. dev. of simulated Im$\{k_z\}$ from physical solution inhomogeneous mesh	$\pm$10 %	n.a.	n.a.	2.69 %	n.a.	n.a.	0.78 %
max. dev. of simulated Re$\{k_x\}$ from physical solution inhomogeneous mesh	$\pm$10 %	3.65 %	0.92 %	5.55 %	0.43 %	0.59 %	0.64 %
NOTE 1 The frequency range $\pm$5 % around the cutoff frequencies can be excluded from the evaluation of the k_z components.							

Table 4: Results of the evaluation of the numerical dispersion characteristics for +y axis and x orientation of the electric field.

Numerical Dispersion Characteristics for $+$Y Axis and Z Orientation of the Electric Field							
	Limit for code compliance	**TE**			**TM**		
ε_r		1	2	2	1	2	2
σ [S/m]		0	0	0.2	0	0	0.2
numerical f_{cutoff} [MHz]		1247	882	<500	1247	882	<500
max. dev. of simulated Re{k_z} from numerical reference homogeneous mesh	±2 %	1.06 %	0.8 %	0.41 %	1.03 %	0.76 %	0.78 %
max. dev. of simulated Im{k_z} from numerical reference homogeneous mesh	±2 %	n.a.	n.a.	1.14 %	n.a.	n.a.	1.24 %
max. dev. of simulated Re{k_x} from numerical reference homogeneous mesh	±2 %	-1.21 %	1.3 %	<0.01 %	-0.36 %	0.4 %	<0.01 %
max. dev. of simulated Re{k_z} from physical solution inhomogeneous mesh	±10 %	-4.71 %	3.63 %	0.92 %	4.65 %	4.29 %	-0.46 %
max. dev. of simulated Im{k_z} from physical solution inhomogeneous mesh	±10 %	n.a.	n.a.	2.69 %	n.a.	n.a.	0.78 %
max. dev. of simulated Re{k_x} from physical solution inhomogeneous mesh	±10 %	5.55 %	0.39 %	5.55 %	0.47 %	0.6 %	0.64 %
NOTE 1 The frequency range ±5 % around the cutoff frequencies can be excluded from the evaluation of the k_z components.							

Table 5: Results of the evaluation of the numerical dispersion characteristics for +y axis and z orientation of the electric field.

Numerical Dispersion Characteristics for $+$Z Axis and X Orientation of the Electric Field							
	Limit for code compliance	**TE**			**TM**		
ε_r		1	2	2	1	2	2
σ [S/m]		0	0	0.2	0	0	0.2
numerical f_{cutoff} [MHz]		1247	882	<500	1247	882	<500
max. dev. of simulated Re{k_z} from numerical reference homogeneous mesh	±2 %	1.04 %	1.3 %	0.78 %	1.05 %	0.74 %	0.78 %
max. dev. of simulated Im{k_z} from numerical reference homogeneous mesh	±2 %	n.a.	n.a.	1.24 %	n.a.	n.a.	1.24 %
max. dev. of simulated Re{k_x} from numerical reference homogeneous mesh	±2 %	-0.54 %	0.04 %	<0.01 %	0.03 %	-0.06 %	<0.01 %
max. dev. of simulated Re{k_z} from physical solution inhomogeneous mesh	±10 %	-4.7 %	3.63 %	0.93 %	4.64 %	4.28 %	-0.46 %
max. dev. of simulated Im{k_z} from physical solution inhomogeneous mesh	±10 %	n.a.	n.a.	2.69 %	n.a.	n.a.	0.78 %
max. dev. of simulated Re{k_x} from physical solution inhomogeneous mesh	±10 %	3.79 %	0.39 %	5.55 %	0.47 %	0.52 %	0.64 %
NOTE 1 The frequency range ±5 % around the cutoff frequencies can be excluded from the evaluation of the k_z components.							

Table 6: Results of the evaluation of the numerical dispersion characteristics for +z axis and x orientation of the electric field.

Numerical Dispersion Characteristics for $+$Z Axis and Y Orientation of the Electric Field							
	Limit for code compliance	**TE**			**TM**		
ε_r		1	2	2	1	2	2
σ [S/m]		0	0	0.2	0	0	0.2
numerical f_{cutoff} [MHz]		1247	882	<500	1247	882	<500
max. dev. of simulated Re{k_z} from numerical reference homogeneous mesh	±2 %	1.05 %	1.3 %	0.78 %	1.03 %	0.74 %	0.78 %
max. dev. of simulated Im{k_z} from numerical reference homogeneous mesh	±2 %	n.a.	n.a.	1.24 %	n.a.	n.a.	1.24 %
max. dev. of simulated Re{k_x} from numerical reference homogeneous mesh	±2 %	0.46 %	-0.81 %	<0.01 %	-0.36 %	-0.3 %	<0.01 %
max. dev. of simulated Re{k_z} from physical solution inhomogeneous mesh	±10 %	-4.69 %	3.63 %	0.93 %	4.65 %	4.29 %	-0.46 %
max. dev. of simulated Im{k_z} from physical solution inhomogeneous mesh	±10 %	n.a.	n.a.	2.69 %	n.a.	n.a.	0.78 %
max. dev. of simulated Re{k_x} from physical solution inhomogeneous mesh	±10 %	8.33 %	0.39 %	5.55 %	0.47 %	0.48 %	0.64 %
NOTE 1 The frequency range ±5 % around the cutoff frequencies can be excluded from the evaluation of the k_z components.							

Table 7: Results of the evaluation of the numerical dispersion characteristics for +z axis and y orientation of the electric field.

Numerical Dispersion Characteristics for $-$X Axis and Y Orientation of the Electric Field							
	Limit for code compliance	**TE**			**TM**		
ε_r		1	2	2	1	2	2
σ [S/m]		0	0	0.2	0	0	0.2
numerical f_{cutoff} [MHz]		1247	882	<500	1247	882	<500
max. dev. of simulated Re{k_z} from numerical reference homogeneous mesh	±2 %	1.07 %	1.3 %	0.78 %	1.08 %	-0.29 %	0.41 %
max. dev. of simulated Im{k_z} from numerical reference homogeneous mesh	±2 %	n.a.	n.a.	1.24 %	n.a.	n.a.	1.14 %
max. dev. of simulated Re{k_x} from numerical reference homogeneous mesh	±2 %	1.16 %	-0.51 %	<0.01 %	-0.76 %	-0.75 %	<0.01 %
max. dev. of simulated Re{k_z} from physical solution inhomogeneous mesh	±10 %	-4.69 %	4.02 %	0.93 %	4.64 %	4.28 %	-0.46 %
max. dev. of simulated Im{k_z} from physical solution inhomogeneous mesh	±10 %	n.a.	n.a.	2.69 %	n.a.	n.a.	0.78 %
max. dev. of simulated Re{k_x} from physical solution inhomogeneous mesh	±10 %	-5.25 %	1.24 %	5.55 %	0.41 %	0.68 %	0.64 %
NOTE 1 The frequency range ±5 % around the cutoff frequencies can be excluded from the evaluation of the k_z components.							

Table 8: Results of the evaluation of the numerical dispersion characteristics for -x axis and y orientation of the electric field.

Numerical Dispersion Characteristics for −X Axis and Z Orientation of the Electric Field							
	Limit for code compliance	**TE**			**TM**		
ε_r		1	2	2	1	2	2
σ [S/m]		0	0	0.2	0	0	0.2
numerical f_{cutoff} [MHz]		1247	882	<500	1247	882	<500
max. dev. of simulated Re{k_z} from numerical reference homogeneous mesh	±2 %	1.14 %	0.81 %	0.41 %	1.06 %	-0.86 %	0.78 %
max. dev. of simulated Im{k_z} from numerical reference homogeneous mesh	±2 %	n.a.	n.a.	1.14 %	n.a.	n.a.	1.24 %
max. dev. of simulated Re{k_x} from numerical reference homogeneous mesh	±2 %	-1.36 %	-0.51 %	<0.01 %	-1.4 %	1.97 %	<0.01 %
max. dev. of simulated Re{k_z} from physical solution inhomogeneous mesh	±10 %	-4.69 %	-7.42 %	0.92 %	4.65 %	4.29 %	-0.46 %
max. dev. of simulated Im{k_z} from physical solution inhomogeneous mesh	±10 %	n.a.	n.a.	2.69 %	n.a.	n.a.	0.78 %
max. dev. of simulated Re{k_x} from physical solution inhomogeneous mesh	±10 %	0.61 %	0.39 %	5.55 %	0.65 %	0.87 %	0.64 %
NOTE 1 The frequency range ±5 % around the cutoff frequencies can be excluded from the evaluation of the k_z components.							

Table 9: Results of the evaluation of the numerical dispersion characteristics for -x axis and z orientation of the electric field.

Numerical Dispersion Characteristics for −Y Axis and X Orientation of the Electric Field							
	Limit for code compliance	**TE**			**TM**		
ε_r		1	2	2	1	2	2
σ [S/m]		0	0	0.2	0	0	0.2
numerical f_{cutoff} [MHz]		1247	882	<500	1247	882	<500
max. dev. of simulated Re{k_z} from numerical reference homogeneous mesh	±2 %	1.07 %	1.3 %	0.78 %	1.08 %	-0.3 %	0.41 %
max. dev. of simulated Im{k_z} from numerical reference homogeneous mesh	±2 %	n.a.	n.a.	1.24 %	n.a.	n.a.	1.14 %
max. dev. of simulated Re{k_x} from numerical reference homogeneous mesh	±2 %	0.03 %	0.04 %	<0.01 %	0.49 %	1.26 %	<0.01 %
max. dev. of simulated Re{k_z} from physical solution inhomogeneous mesh	±10 %	-4.69 %	3.97 %	0.93 %	4.65 %	4.3 %	-0.46 %
max. dev. of simulated Im{k_z} from physical solution inhomogeneous mesh	±10 %	n.a.	n.a.	2.69 %	n.a.	n.a.	0.78 %
max. dev. of simulated Re{k_x} from physical solution inhomogeneous mesh	±10 %	-5.01 %	0.46 %	5.55 %	0.41 %	0.71 %	0.64 %
NOTE 1 The frequency range ±5 % around the cutoff frequencies can be excluded from the evaluation of the k_z components.							

Table 10: Results of the evaluation of the numerical dispersion characteristics for -y axis and x orientation of the electric field.

Numerical Dispersion Characteristics for $-$Y Axis and Z Orientation of the Electric Field							
	Limit for code compliance	**TE**			**TM**		
ε_r		1	2	2	1	2	2
σ [S/m]		0	0	0.2	0	0	0.2
numerical f_{cutoff} [MHz]		1247	882	<500	1247	882	<500
max. dev. of simulated Re$\{k_z\}$ from numerical reference homogeneous mesh	$\pm$2 %	1.06 %	0.8 %	0.41 %	1.06 %	0.74 %	0.78 %
max. dev. of simulated Im$\{k_z\}$ from numerical reference homogeneous mesh	$\pm$2 %	n.a.	n.a.	1.14 %	n.a.	n.a.	1.24 %
max. dev. of simulated Re$\{k_x\}$ from numerical reference homogeneous mesh	$\pm$2 %	-1.21 %	1.3 %	<0.01 %	-0.55 %	-0.3 %	<0.01 %
max. dev. of simulated Re$\{k_z\}$ from physical solution inhomogeneous mesh	$\pm$10 %	-4.69 %	3.63 %	0.92 %	4.65 %	4.3 %	-0.46 %
max. dev. of simulated Im$\{k_z\}$ from physical solution inhomogeneous mesh	$\pm$10 %	n.a.	n.a.	2.69 %	n.a.	n.a.	0.78 %
max. dev. of simulated Re$\{k_x\}$ from physical solution inhomogeneous mesh	$\pm$10 %	-6.23 %	0.4 %	5.55 %	0.51 %	0.69 %	0.64 %
NOTE 1 The frequency range $\pm$5 % around the cutoff frequencies can be excluded from the evaluation of the k_z components.							

Table 11: Results of the evaluation of the numerical dispersion characteristics for -y axis and z orientation of the electric field.

Numerical Dispersion Characteristics for $-$Z Axis and X Orientation of the Electric Field							
	Limit for code compliance	**TE**			**TM**		
ε_r		1	2	2	1	2	2
σ [S/m]		0	0	0.2	0	0	0.2
numerical f_{cutoff} [MHz]		1247	882	<500	1247	882	<500
max. dev. of simulated Re$\{k_z\}$ from numerical reference homogeneous mesh	$\pm$2 %	1.05 %	1.29 %	0.78 %	n.a.	0.74 %	0.78 %
max. dev. of simulated Im$\{k_z\}$ from numerical reference homogeneous mesh	$\pm$2 %	n.a.	n.a.	1.24 %	n.a.	n.a.	1.24 %
max. dev. of simulated Re$\{k_x\}$ from numerical reference homogeneous mesh	$\pm$2 %	0.03 %	0.05 %	<0.01 %	n.a.	-0.06 %	<0.01 %
max. dev. of simulated Re$\{k_z\}$ from physical solution inhomogeneous mesh	$\pm$10 %	-4.69 %	3.63 %	0.93 %	4.64 %	4.28 %	-0.46 %
max. dev. of simulated Im$\{k_z\}$ from physical solution inhomogeneous mesh	$\pm$10 %	n.a.	n.a.	2.69 %	n.a.	n.a.	0.78 %
max. dev. of simulated Re$\{k_x\}$ from physical solution inhomogeneous mesh	$\pm$10 %	8.22 %	0.39 %	5.55 %	0.47 %	0.52 %	0.64 %
NOTE 1 The frequency range $\pm$5 % around the cutoff frequencies can be excluded from the evaluation of the k_z components.							

Table 12: Results of the evaluation of the numerical dispersion characteristics for -z axis and x orientation of the electric field.

Numerical Dispersion Characteristics for $-$Z Axis and Y Orientation of the Electric Field							
	Limit for code compliance	**TE**			**TM**		
ε_r		1	2	2	1	2	2
σ [S/m]		0	0	0.2	0	0	0.2
numerical f_{cutoff} [MHz]		1247	882	<500	1247	882	<500
max. dev. of simulated Re$\{k_z\}$ from numerical reference homogeneous mesh	$\pm$2 %	1.05 %	1.3 %	0.78 %	1.06 %	0.76 %	0.78 %
max. dev. of simulated Im$\{k_z\}$ from numerical reference homogeneous mesh	$\pm$2 %	n.a.	n.a.	1.24 %	n.a.	n.a.	1.24 %
max. dev. of simulated Re$\{k_x\}$ from numerical reference homogeneous mesh	$\pm$2 %	0.46 %	-0.81 %	<0.01 %	-0.55 %	0.4 %	<0.01 %
max. dev. of simulated Re$\{k_z\}$ from physical solution inhomogeneous mesh	$\pm$10 %	-4.69 %	3.63 %	0.93 %	4.65 %	4.3 %	-0.46 %
max. dev. of simulated Im$\{k_z\}$ from physical solution inhomogeneous mesh	$\pm$10 %	n.a.	n.a.	2.69 %	n.a.	n.a.	0.78 %
max. dev. of simulated Re$\{k_x\}$ from physical solution inhomogeneous mesh	$\pm$10 %	8.33 %	0.39 %	5.55 %	0.51 %	0.51 %	0.64 %
NOTE 1 The frequency range $\pm$5 % around the cutoff frequencies can be excluded from the evaluation of the k_z components.							

Table 13: Results of the evaluation of the numerical dispersion characteristics for -z axis and y orientation of the electric field.

2.2 Planar Dielectric Boundaries

The simulation model has been set up as defined in section 8.2.2 of IEC/IEEE 62704-1. This section shows the maximum deviation of the wave number in dielectric and the reflection from the references.

Numerical Reflection Coefficient for +X Axis and Y Orientation of the Electric Field				
	Limit for code compliance	**TE**		**TM**
ε_r		4	4	4
σ [S/m]		0	0.2	0
max. dev. of simulated Re$\{k_{2z}\}$ from numerical reference 1.3 GHz $<$ f $<$ 2 GHz	$\pm$5 %	0.95 %	2.48 %	0.95 %
max. dev. of simulated Im$\{k_{2z}\}$ from numerical reference 0.5 GHz $<$ f $<$ 0,6 GHz	$\pm$5 %	n.a.	0.2 %	n.a.
max. dev. of simulated Re$\{r\}$ from numerical reference 1.3 GHz $<$ f $<$ 2 GHz	$\pm$5 %	<0.01 %	<0.01 %	0.04 %
max. dev. of simulated Im$\{r\}$ from numerical reference 1.3 GHz $<$ f $<$ 2 GHz	$\pm$5 %	n.a.	<0.01 %	n.a.
max. dev. of simulated Re$\{r\}$ from numerical reference 0.5 GHz $<$ f $<$ 0,6 GHz	$\pm$10 %	-0.02 %	<0.01 %	0.04 %
max. dev. of simulated Im$\{r\}$ from numerical reference 0.5 GHz $<$ f $<$ 0,6 GHz	$\pm$10 %	n.a.	<0.01 %	n.a.
NOTE 1 Larger tolerances apply for the deviation of the simulation from the reference for frequencies below cut-off.				

Table 14: Results of the evaluation of the numerical reflection coefficient for +x axis and y orientation of the electric field.

Numerical Reflection Coefficient for +X Axis and Z Orientation of the Electric Field				
	Limit for code compliance	**TE**		**TM**
ε_r		4	4	4
σ [S/m]		0	0.2	0
max. dev. of simulated Re$\{k_{2z}\}$ from numerical reference 1.3 GHz $<$ f $<$ 2 GHz	$\pm$5 %	0.95 %	2.48 %	0.95 %
max. dev. of simulated Im$\{k_{2z}\}$ from numerical reference 0.5 GHz $<$ f $<$ 0,6 GHz	$\pm$5 %	n.a.	0.2 %	n.a.
max. dev. of simulated Re$\{r\}$ from numerical reference 1.3 GHz $<$ f $<$ 2 GHz	$\pm$5 %	<0.01 %	<0.01 %	0.04 %
max. dev. of simulated Im$\{r\}$ from numerical reference 1.3 GHz $<$ f $<$ 2 GHz	$\pm$5 %	n.a.	<0.01 %	n.a.
max. dev. of simulated Re$\{r\}$ from numerical reference 0.5 GHz $<$ f $<$ 0,6 GHz	$\pm$10 %	-0.02 %	<0.01 %	0.06 %
max. dev. of simulated Im$\{r\}$ from numerical reference 0.5 GHz $<$ f $<$ 0,6 GHz	$\pm$10 %	n.a.	<0.01 %	n.a.
NOTE 1 Larger tolerances apply for the deviation of the simulation from the reference for frequencies below cut-off.				

Table 15: Results of the evaluation of the numerical reflection coefficient for +x axis and z orientation of the electric field.

Numerical Reflection Coefficient for +Y Axis and X Orientation of the Electric Field				
	Limit for code compliance	**TE**		**TM**
ε_r		4	4	4
σ [S/m]		0	0.2	0
max. dev. of simulated Re$\{k_{2z}\}$ from numerical reference 1.3 GHz $<$ f $<$ 2 GHz	$\pm$5 %	0.95 %	2.48 %	0.95 %
max. dev. of simulated Im$\{k_{2z}\}$ from numerical reference 0.5 GHz $<$ f $<$ 0,6 GHz	$\pm$5 %	n.a.	0.2 %	n.a.
max. dev. of simulated Re$\{r\}$ from numerical reference 1.3 GHz $<$ f $<$ 2 GHz	$\pm$5 %	<0.01 %	<0.01 %	0.04 %
max. dev. of simulated Im$\{r\}$ from numerical reference 1.3 GHz $<$ f $<$ 2 GHz	$\pm$5 %	n.a.	<0.01 %	n.a.
max. dev. of simulated Re$\{r\}$ from numerical reference 0.5 GHz $<$ f $<$ 0,6 GHz	$\pm$10 %	0.03 %	<0.01 %	0.03 %
max. dev. of simulated Im$\{r\}$ from numerical reference 0.5 GHz $<$ f $<$ 0,6 GHz	$\pm$10 %	n.a.	<0.01 %	n.a.
NOTE 1 Larger tolerances apply for the deviation of the simulation from the reference for frequencies below cut-off.				

Table 16: Results of the evaluation of the numerical reflection coefficient for +y axis and x orientation of the electric field.

IMST

Numerical Reflection Coefficient for +Y Axis and Z Orientation of the Electric Field				
	Limit for code compliance	**TE**		**TM**
ε_r		4	4	4
σ [S/m]		0	0.2	0
max. dev. of simulated Re$\{k_{2z}\}$ from numerical reference 1.3 GHz $<$ f $<$ 2 GHz	±5 %	0.95 %	2.48 %	0.95 %
max. dev. of simulated Im$\{k_{2z}\}$ from numerical reference 0.5 GHz $<$ f $<$ 0,6 GHz	±5 %	n.a.	0.2 %	n.a.
max. dev. of simulated Re$\{r\}$ from numerical reference 1.3 GHz $<$ f $<$ 2 GHz	±5 %	<0.01 %	<0.01 %	0.04 %
max. dev. of simulated Im$\{r\}$ from numerical reference 1.3 GHz $<$ f $<$ 2 GHz	±5 %	n.a.	<0.01 %	n.a.
max. dev. of simulated Re$\{r\}$ from numerical reference 0.5 GHz $<$ f $<$ 0,6 GHz	±10 %	-0.01 %	<0.01 %	0.03 %
max. dev. of simulated Im$\{r\}$ from numerical reference 0.5 GHz $<$ f $<$ 0,6 GHz	±10 %	n.a.	<0.01 %	n.a.
NOTE 1 Larger tolerances apply for the deviation of the simulation from the reference for frequencies below cut-off.				

Table 17: Results of the evaluation of the numerical reflection coefficient for +y axis and z orientation of the electric field.

Numerical Reflection Coefficient for +Z Axis and X Orientation of the Electric Field				
	Limit for code compliance	**TE**		**TM**
ε_r		4	4	4
σ [S/m]		0	0.2	0
max. dev. of simulated Re$\{k_{2z}\}$ from numerical reference 1.3 GHz $<$ f $<$ 2 GHz	±5 %	0.95 %	2.48 %	0.95 %
max. dev. of simulated Im$\{k_{2z}\}$ from numerical reference 0.5 GHz $<$ f $<$ 0,6 GHz	±5 %	n.a.	0.2 %	n.a.
max. dev. of simulated Re$\{r\}$ from numerical reference 1.3 GHz $<$ f $<$ 2 GHz	±5 %	<0.01 %	<0.01 %	0.03 %
max. dev. of simulated Im$\{r\}$ from numerical reference 1.3 GHz $<$ f $<$ 2 GHz	±5 %	n.a.	<0.01 %	n.a.
max. dev. of simulated Re$\{r\}$ from numerical reference 0.5 GHz $<$ f $<$ 0,6 GHz	±10 %	0.03 %	<0.01 %	0.02 %
max. dev. of simulated Im$\{r\}$ from numerical reference 0.5 GHz $<$ f $<$ 0,6 GHz	±10 %	n.a.	<0.01 %	n.a.
NOTE 1 Larger tolerances apply for the deviation of the simulation from the reference for frequencies below cut-off.				

Table 18: Results of the evaluation of the numerical reflection coefficient for +z axis and x orientation of the electric field.

Numerical Reflection Coefficient for +Z Axis and Y Orientation of the Electric Field				
	Limit for code compliance	**TE**		**TM**
ε_r		4	4	4
σ [S/m]		0	0.2	0
max. dev. of simulated Re$\{k_{2z}\}$ from numerical reference 1.3 GHz $<$ f $<$ 2 GHz	$\pm$5 %	0.95 %	2.48 %	0.95 %
max. dev. of simulated Im$\{k_{2z}\}$ from numerical reference 0.5 GHz $<$ f $<$ 0,6 GHz	$\pm$5 %	n.a.	0.2 %	n.a.
max. dev. of simulated Re$\{r\}$ from numerical reference 1.3 GHz $<$ f $<$ 2 GHz	$\pm$5 %	<0.01 %	<0.01 %	0.05 %
max. dev. of simulated Im$\{r\}$ from numerical reference 1.3 GHz $<$ f $<$ 2 GHz	$\pm$5 %	n.a.	<0.01 %	n.a.
max. dev. of simulated Re$\{r\}$ from numerical reference 0.5 GHz $<$ f $<$ 0,6 GHz	$\pm$10 %	0.05 %	<0.01 %	0.03 %
max. dev. of simulated Im$\{r\}$ from numerical reference 0.5 GHz $<$ f $<$ 0,6 GHz	$\pm$10 %	n.a.	<0.01 %	n.a.
NOTE 1 Larger tolerances apply for the deviation of the simulation from the reference for frequencies below cut-off.				

Table 19: Results of the evaluation of the numerical reflection coefficient for +z axis and y orientation of the electric field.

Numerical Reflection Coefficient for -X Axis and Y Orientation of the Electric Field				
	Limit for code compliance	**TE**		**TM**
ε_r		4	4	4
σ [S/m]		0	0.2	0
max. dev. of simulated Re$\{k_{2z}\}$ from numerical reference 1.3 GHz $<$ f $<$ 2 GHz	$\pm$5 %	0.95 %	2.48 %	0.95 %
max. dev. of simulated Im$\{k_{2z}\}$ from numerical reference 0.5 GHz $<$ f $<$ 0,6 GHz	$\pm$5 %	n.a.	0.2 %	n.a.
max. dev. of simulated Re$\{r\}$ from numerical reference 1.3 GHz $<$ f $<$ 2 GHz	$\pm$5 %	<0.01 %	<0.01 %	0.04 %
max. dev. of simulated Im$\{r\}$ from numerical reference 1.3 GHz $<$ f $<$ 2 GHz	$\pm$5 %	n.a.	<0.01 %	n.a.
max. dev. of simulated Re$\{r\}$ from numerical reference 0.5 GHz $<$ f $<$ 0,6 GHz	$\pm$10 %	-0.02 %	<0.01 %	0.04 %
max. dev. of simulated Im$\{r\}$ from numerical reference 0.5 GHz $<$ f $<$ 0,6 GHz	$\pm$10 %	n.a.	<0.01 %	n.a.
NOTE 1 Larger tolerances apply for the deviation of the simulation from the reference for frequencies below cut-off.				

Table 20: Results of the evaluation of the numerical reflection coefficient for -x axis and y orientation of the electric field.

Numerical Reflection Coefficient for -X Axis and Z Orientation of the Electric Field				
	Limit for code compliance	**TE**		**TM**
ε_r		4	4	4
σ [S/m]		0	0.2	0
max. dev. of simulated Re$\{k_{2z}\}$ from numerical reference 1.3 GHz $<$ f $<$ 2 GHz	±5 %	0.95 %	2.48 %	0.95 %
max. dev. of simulated Im$\{k_{2z}\}$ from numerical reference 0.5 GHz $<$ f $<$ 0,6 GHz	±5 %	n.a.	0.2 %	n.a.
max. dev. of simulated Re$\{r\}$ from numerical reference 1.3 GHz $<$ f $<$ 2 GHz	±5 %	<0.01 %	<0.01 %	0.03 %
max. dev. of simulated Im$\{r\}$ from numerical reference 1.3 GHz $<$ f $<$ 2 GHz	±5 %	n.a.	<0.01 %	n.a.
max. dev. of simulated Re$\{r\}$ from numerical reference 0.5 GHz $<$ f $<$ 0,6 GHz	±10 %	-0.02 %	<0.01 %	0.03 %
max. dev. of simulated Im$\{r\}$ from numerical reference 0.5 GHz $<$ f $<$ 0,6 GHz	±10 %	n.a.	<0.01 %	n.a.
NOTE 1 Larger tolerances apply for the deviation of the simulation from the reference for frequencies below cut-off.				

Table 21: Results of the evaluation of the numerical reflection coefficient for -x axis and z orientation of the electric field.

Numerical Reflection Coefficient for -Y Axis and X Orientation of the Electric Field				
	Limit for code compliance	**TE**		**TM**
ε_r		4	4	4
σ [S/m]		0	0.2	0
max. dev. of simulated Re$\{k_{2z}\}$ from numerical reference 1.3 GHz $<$ f $<$ 2 GHz	±5 %	0.95 %	2.48 %	0.95 %
max. dev. of simulated Im$\{k_{2z}\}$ from numerical reference 0.5 GHz $<$ f $<$ 0,6 GHz	±5 %	n.a.	0.2 %	n.a.
max. dev. of simulated Re$\{r\}$ from numerical reference 1.3 GHz $<$ f $<$ 2 GHz	±5 %	<0.01 %	<0.01 %	0.04 %
max. dev. of simulated Im$\{r\}$ from numerical reference 1.3 GHz $<$ f $<$ 2 GHz	±5 %	n.a.	<0.01 %	n.a.
max. dev. of simulated Re$\{r\}$ from numerical reference 0.5 GHz $<$ f $<$ 0,6 GHz	±10 %	0.03 %	<0.01 %	0.03 %
max. dev. of simulated Im$\{r\}$ from numerical reference 0.5 GHz $<$ f $<$ 0,6 GHz	±10 %	n.a.	<0.01 %	n.a.
NOTE 1 Larger tolerances apply for the deviation of the simulation from the reference for frequencies below cut-off.				

Table 22: Results of the evaluation of the numerical reflection coefficient for -y axis and x orientation of the electric field.

Numerical Reflection Coefficient for -Y Axis and X Orientation of the Electric Field				
	Limit for code compliance	**TE**		**TM**
ε_r		4	4	4
σ [S/m]		0	0.2	0
max. dev. of simulated Re$\{k_{2z}\}$ from numerical reference 1.3 GHz $<$ f $<$ 2 GHz	$\pm$5 %	0.95 %	2.48 %	0.95 %
max. dev. of simulated Im$\{k_{2z}\}$ from numerical reference 0.5 GHz $<$ f $<$ 0,6 GHz	$\pm$5 %	n.a.	0.2 %	n.a.
max. dev. of simulated Re$\{r\}$ from numerical reference 1.3 GHz $<$ f $<$ 2 GHz	$\pm$5 %	<0.01 %	<0.01 %	0.05 %
max. dev. of simulated Im$\{r\}$ from numerical reference 1.3 GHz $<$ f $<$ 2 GHz	$\pm$5 %	n.a.	<0.01 %	n.a.
max. dev. of simulated Re$\{r\}$ from numerical reference 0.5 GHz $<$ f $<$ 0,6 GHz	$\pm$10 %	-0.01 %	<0.01 %	0.03 %
max. dev. of simulated Im$\{r\}$ from numerical reference 0.5 GHz $<$ f $<$ 0,6 GHz	$\pm$10 %	n.a.	<0.01 %	n.a.
NOTE 1 Larger tolerances apply for the deviation of the simulation from the reference for frequencies below cut-off.				

Table 23: Results of the evaluation of the numerical reflection coefficient for -y axis and z orientation of the electric field.

Numerical Reflection Coefficient for -Z Axis and X Orientation of the Electric Field				
	Limit for code compliance	**TE**		**TM**
ε_r		4	4	4
σ [S/m]		0	0.2	0
max. dev. of simulated Re$\{k_{2z}\}$ from numerical reference 1.3 GHz $<$ f $<$ 2 GHz	$\pm$5 %	0.95 %	2.48 %	0.95 %
max. dev. of simulated Im$\{k_{2z}\}$ from numerical reference 0.5 GHz $<$ f $<$ 0,6 GHz	$\pm$5 %	n.a.	0.2 %	n.a.
max. dev. of simulated Re$\{r\}$ from numerical reference 1.3 GHz $<$ f $<$ 2 GHz	$\pm$5 %	<0.01 %	<0.01 %	0.03 %
max. dev. of simulated Im$\{r\}$ from numerical reference 1.3 GHz $<$ f $<$ 2 GHz	$\pm$5 %	n.a.	<0.01 %	n.a.
max. dev. of simulated Re$\{r\}$ from numerical reference 0.5 GHz $<$ f $<$ 0,6 GHz	$\pm$10 %	0.03 %	<0.01 %	0.02 %
max. dev. of simulated Im$\{r\}$ from numerical reference 0.5 GHz $<$ f $<$ 0,6 GHz	$\pm$10 %	n.a.	<0.01 %	n.a.
NOTE 1 Larger tolerances apply for the deviation of the simulation from the reference for frequencies below cut-off.				

Table 24: Results of the evaluation of the numerical reflection coefficient for -z axis and x orientation of the electric field.

Numerical Reflection Coefficient for -Z Axis and Y Orientation of the Electric Field				
	Limit for code compliance	**TE**		**TM**
ε_r		4	4	4
σ [S/m]		0	0.2	0
max. dev. of simulated Re{k_{2z}} from numerical reference 1.3 GHz $<$ f $<$ 2 GHz	±5 %	0.95 %	2.48 %	0.95 %
max. dev. of simulated Im{k_{2z}} from numerical reference 0.5 GHz $<$ f $<$ 0,6 GHz	±5 %	n.a.	0.2 %	n.a.
max. dev. of simulated Re{r} from numerical reference 1.3 GHz $<$ f $<$ 2 GHz	±5 %	<0.01 %	<0.01 %	0.04 %
max. dev. of simulated Im{r} from numerical reference 1.3 GHz $<$ f $<$ 2 GHz	±5 %	n.a.	<0.01 %	n.a.
max. dev. of simulated Re{r} from numerical reference 0.5 GHz $<$ f $<$ 0,6 GHz	±10 %	0.05 %	<0.01 %	0.03 %
max. dev. of simulated Im{r} from numerical reference 0.5 GHz $<$ f $<$ 0,6 GHz	±10 %	n.a.	<0.01 %	n.a.
NOTE 1 Larger tolerances apply for the deviation of the simulation from the reference for frequencies below cut-off.				

Table 25: Results of the evaluation of the numerical reflection coefficient for -z axis and y orientation of the electric field.

2.3 Absorbing Boundary Conditions

2.3.1 Aligned absorbing boundary conditions

The simulation model has been set up as defined in section 8.2.3.1 of IEC/IEEE 62704-1. This section shows the power reflection coefficient in the range of 0.5 to 3 GHz in the permissible range (grey).

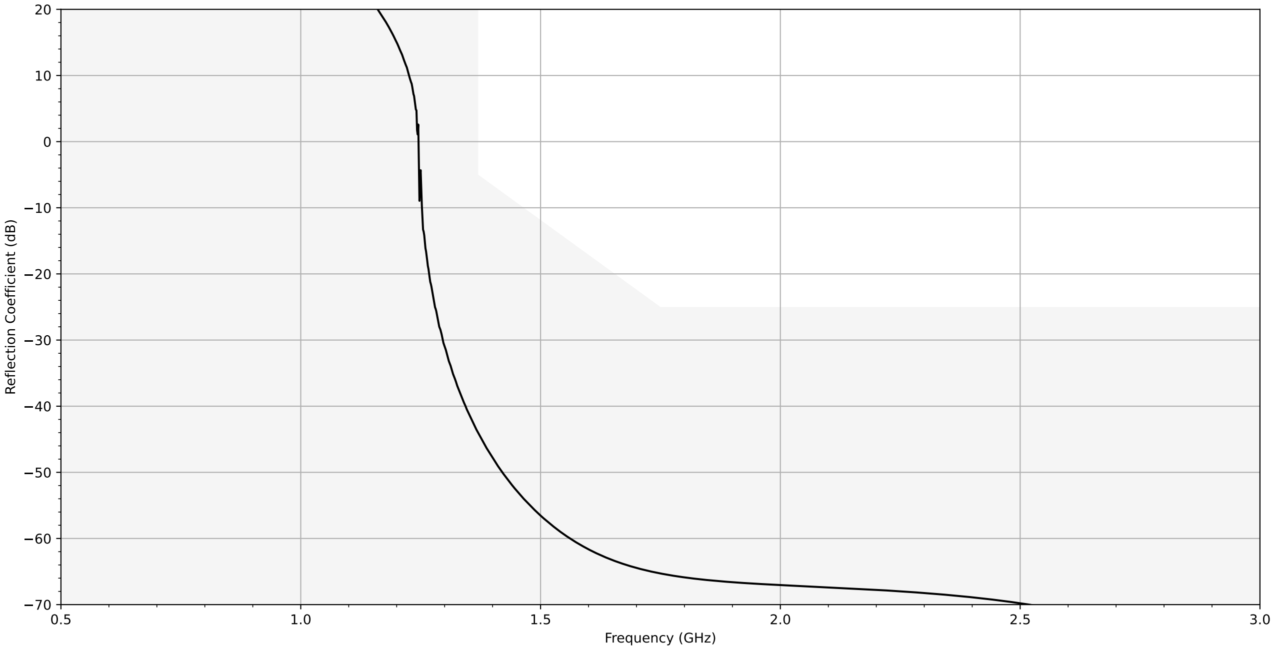

Figure 1: Reflection coefficient for TE, x-axis, y-pol, homogen. mesh

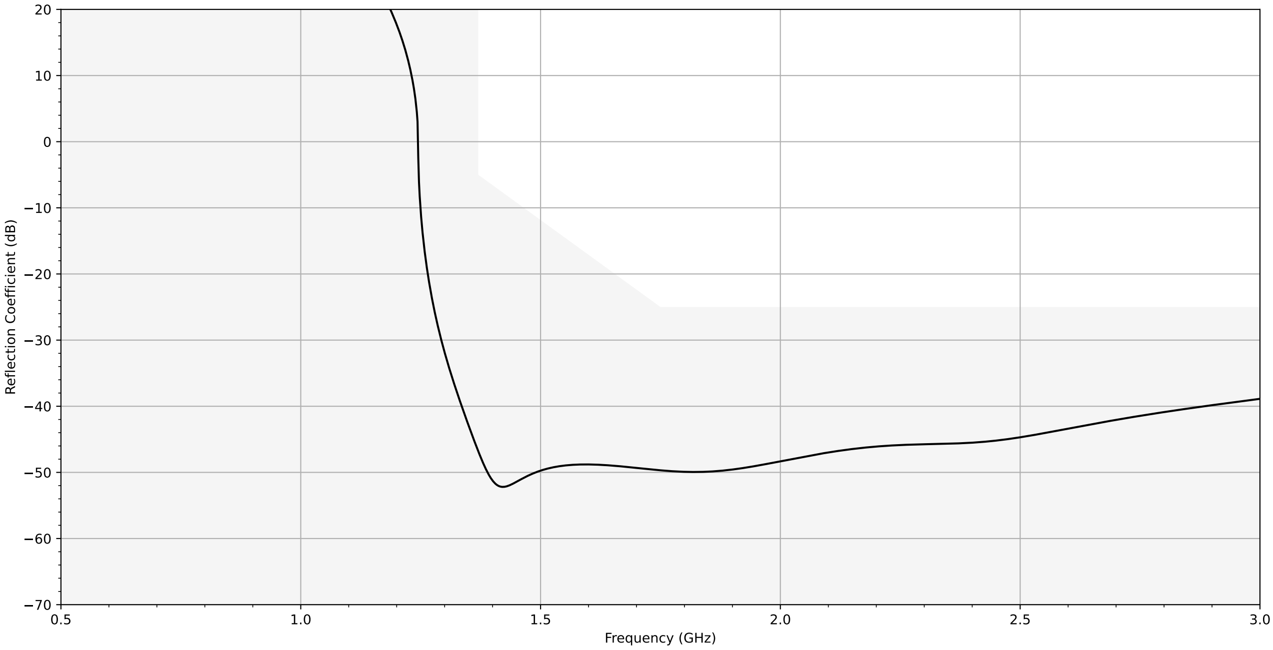

Figure 2: Reflection coefficient for TE, x-axis, y-pol, inhomogen. mesh

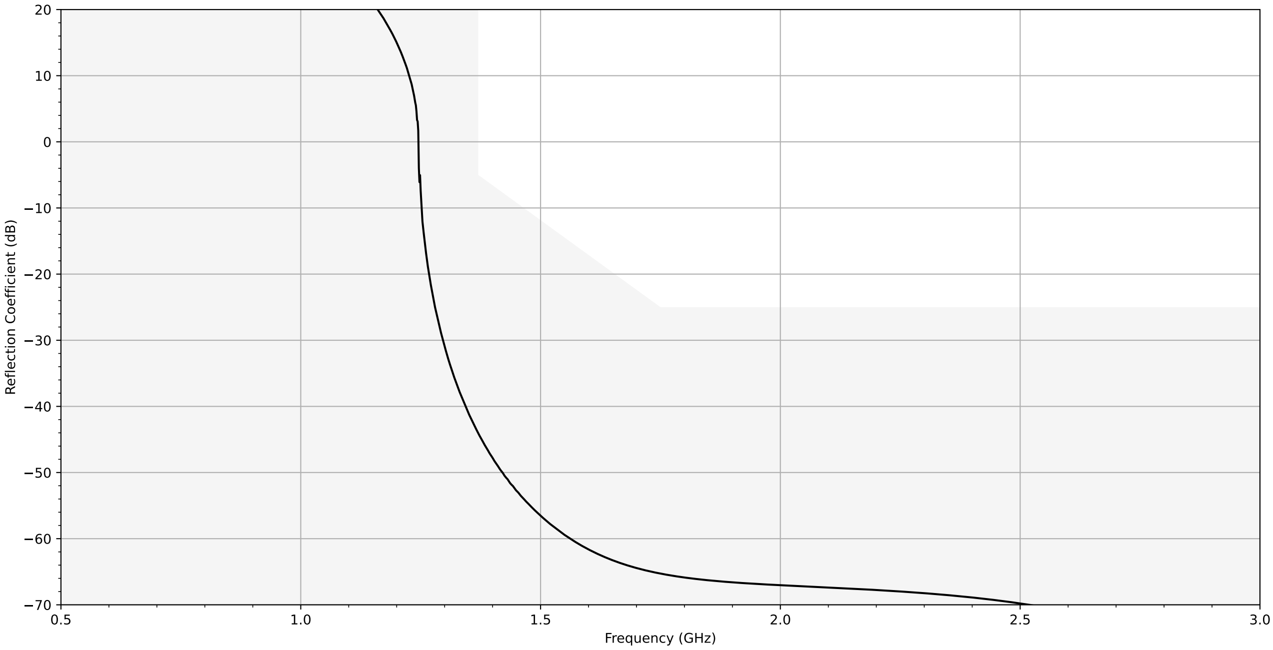

Figure 3: Reflection coefficient for TE, x-axis, z-pol, homogen. mesh

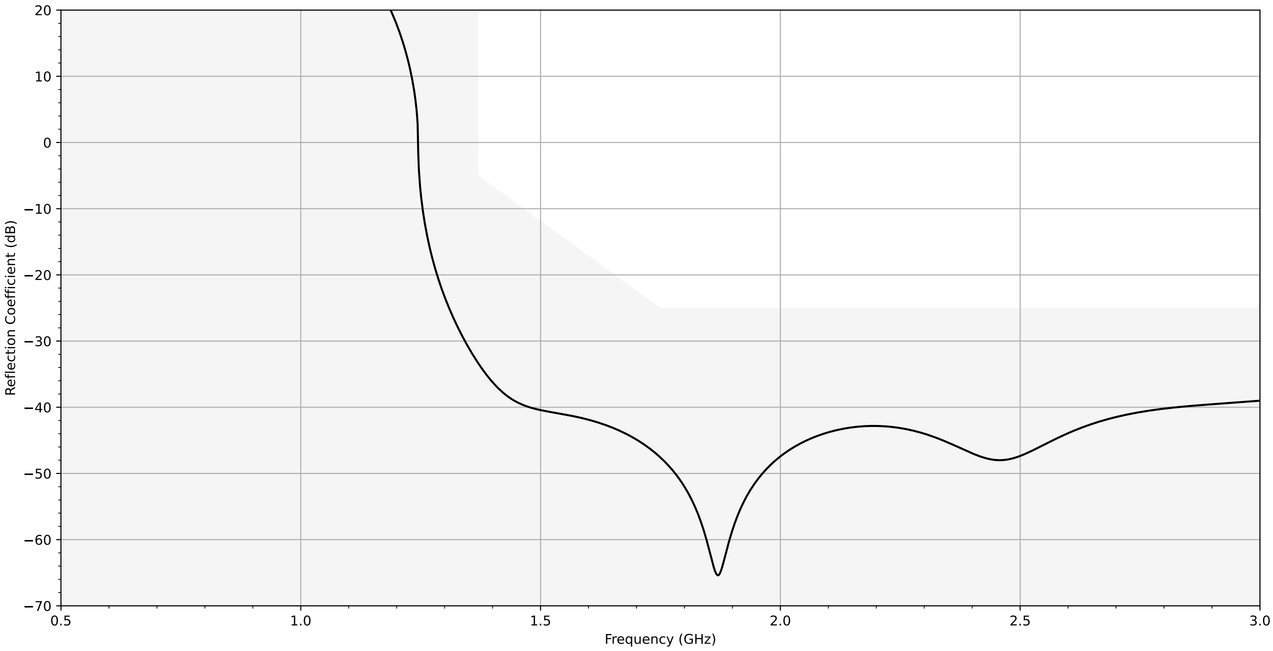

Figure 4: Reflection coefficient for TE, x-axis, z-pol, inhomogen. mesh

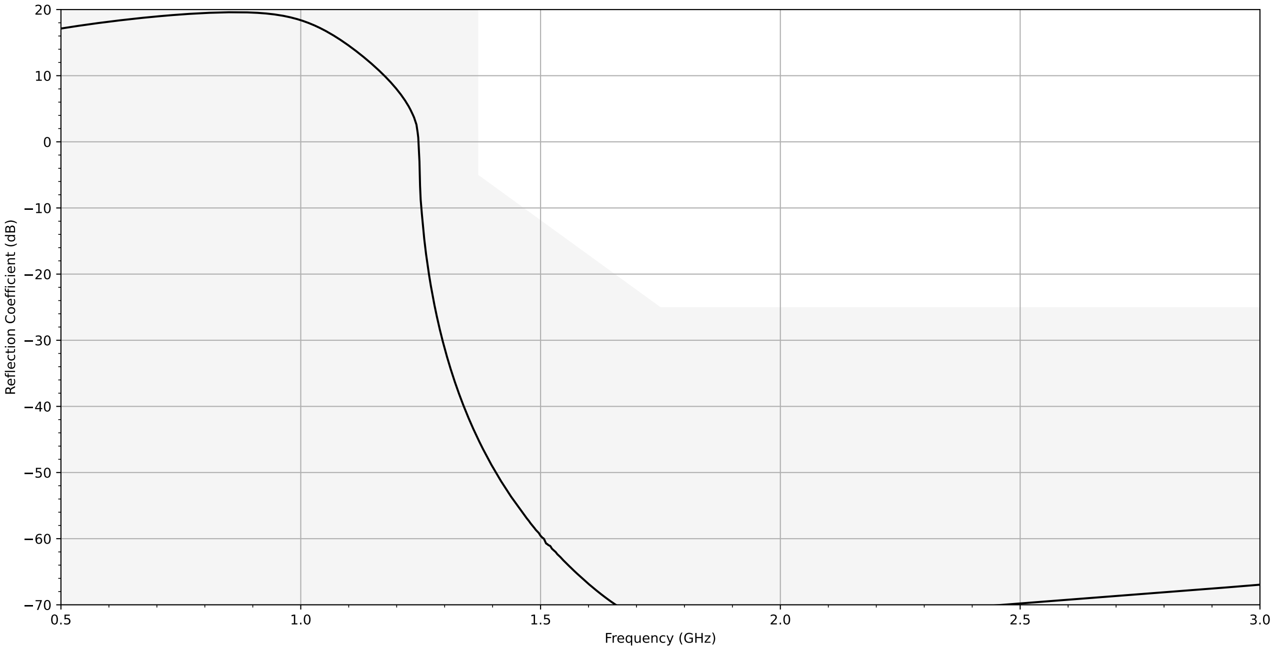

Figure 5: Reflection coefficient for TE, y-axis, x-pol, homogen. mesh

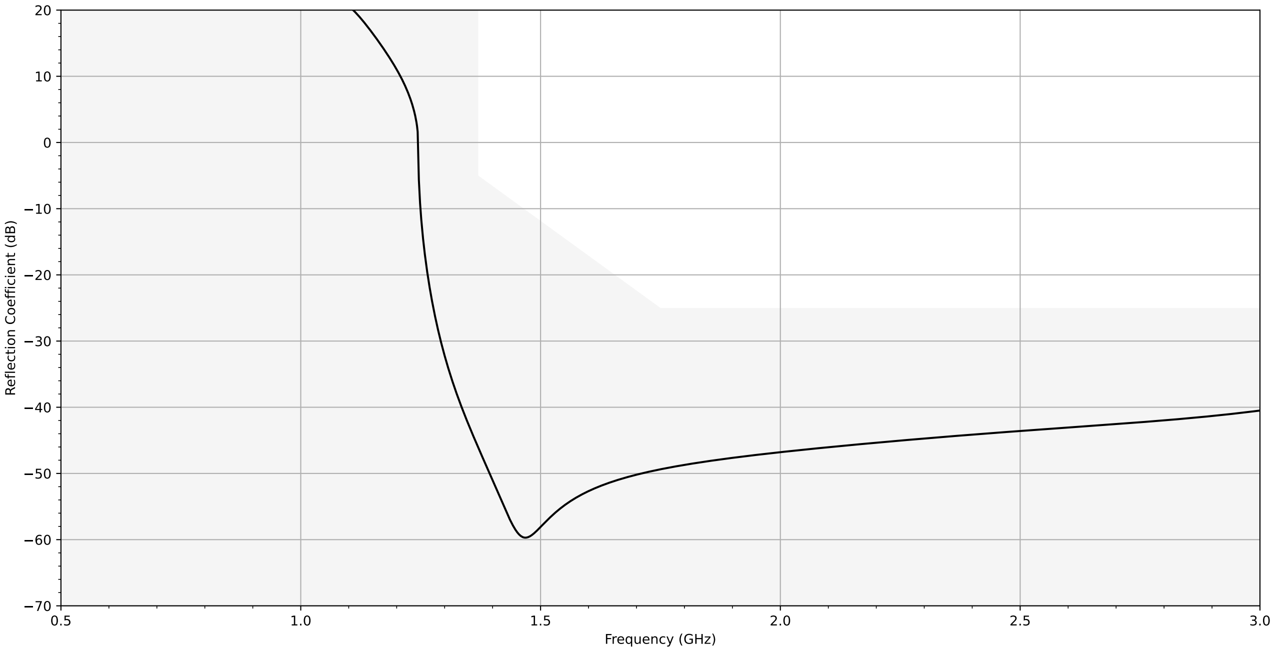

Figure 6: Reflection coefficient for TE, y-axis, x-pol, inhomogen. mesh

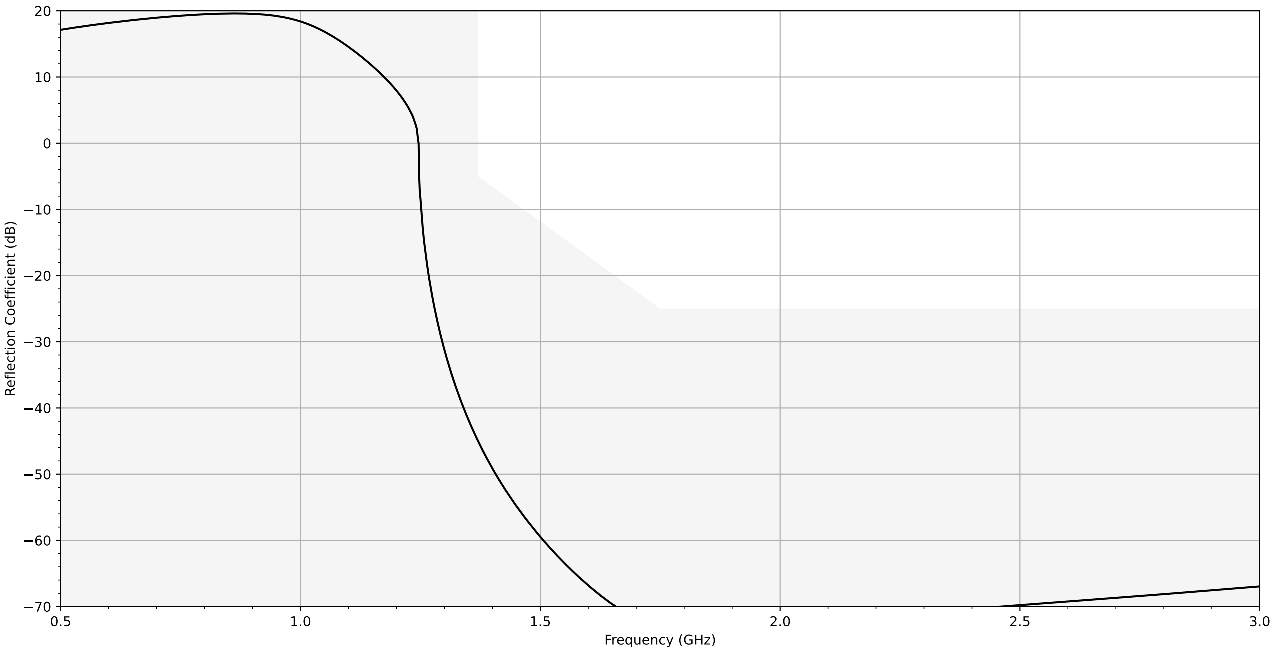

Figure 7: Reflection coefficient for TE, y-axis, z-pol, homogen. mesh

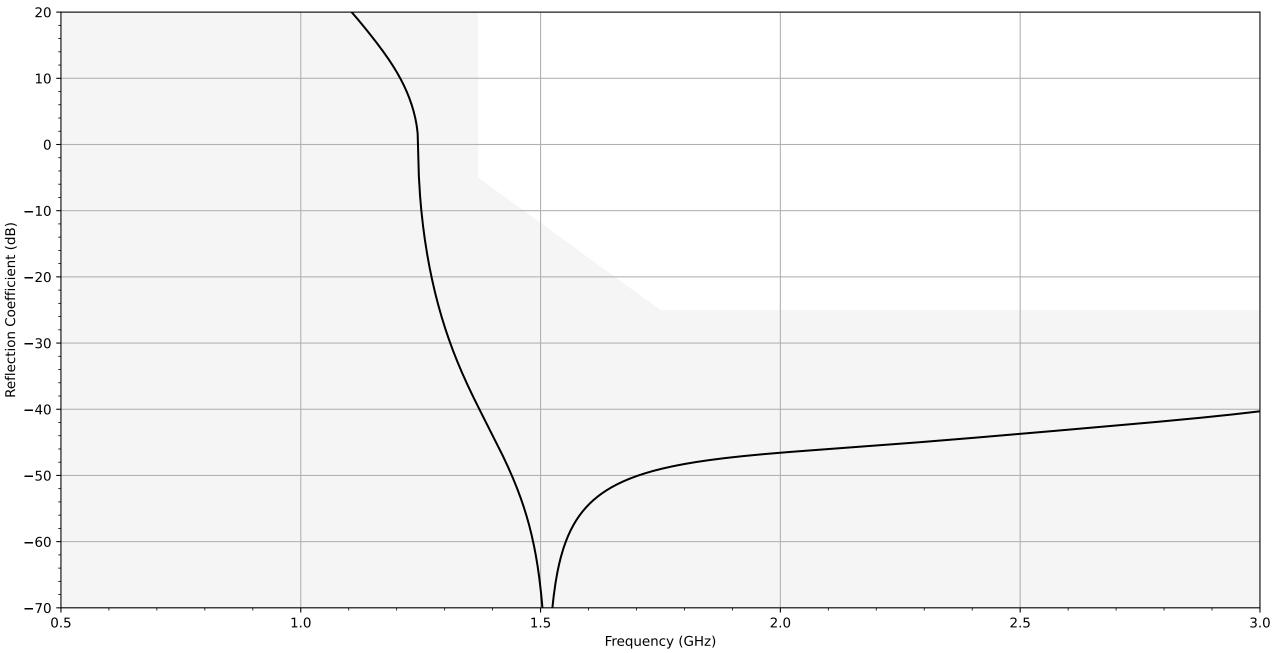

Figure 8: Reflection coefficient for TE, y-axis, z-pol, inhomogen. mesh

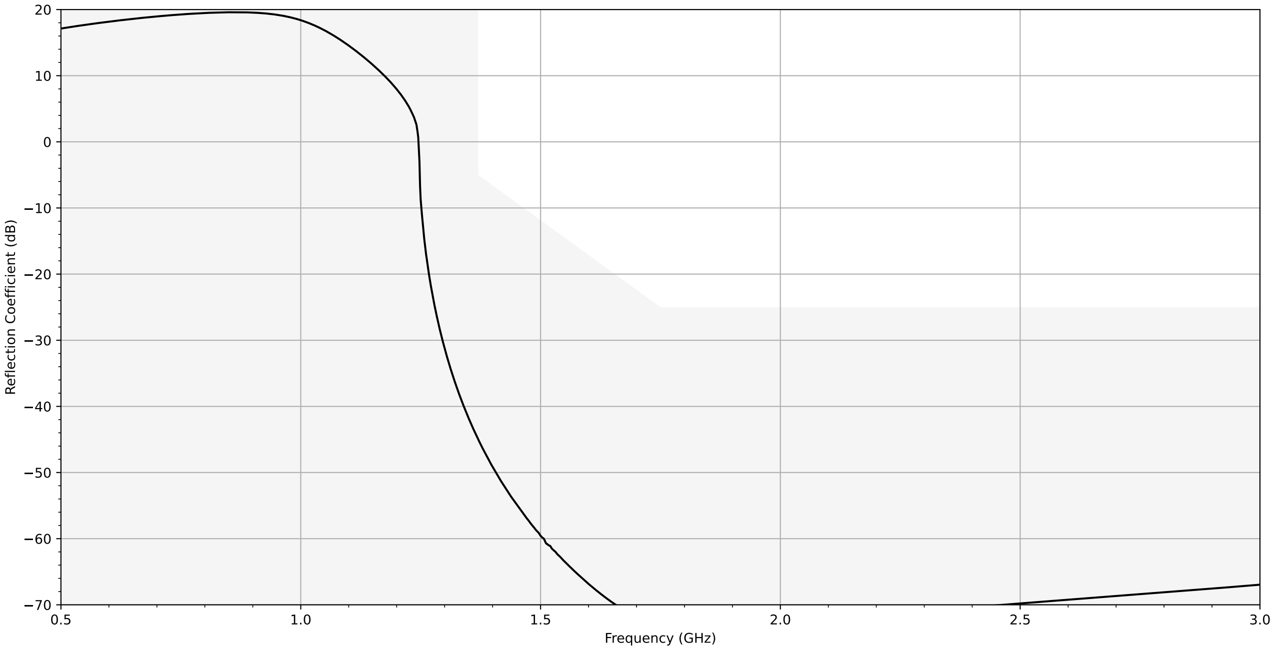

Figure 9: Reflection coefficient for TE, z-axis, x-pol, homogen. mesh

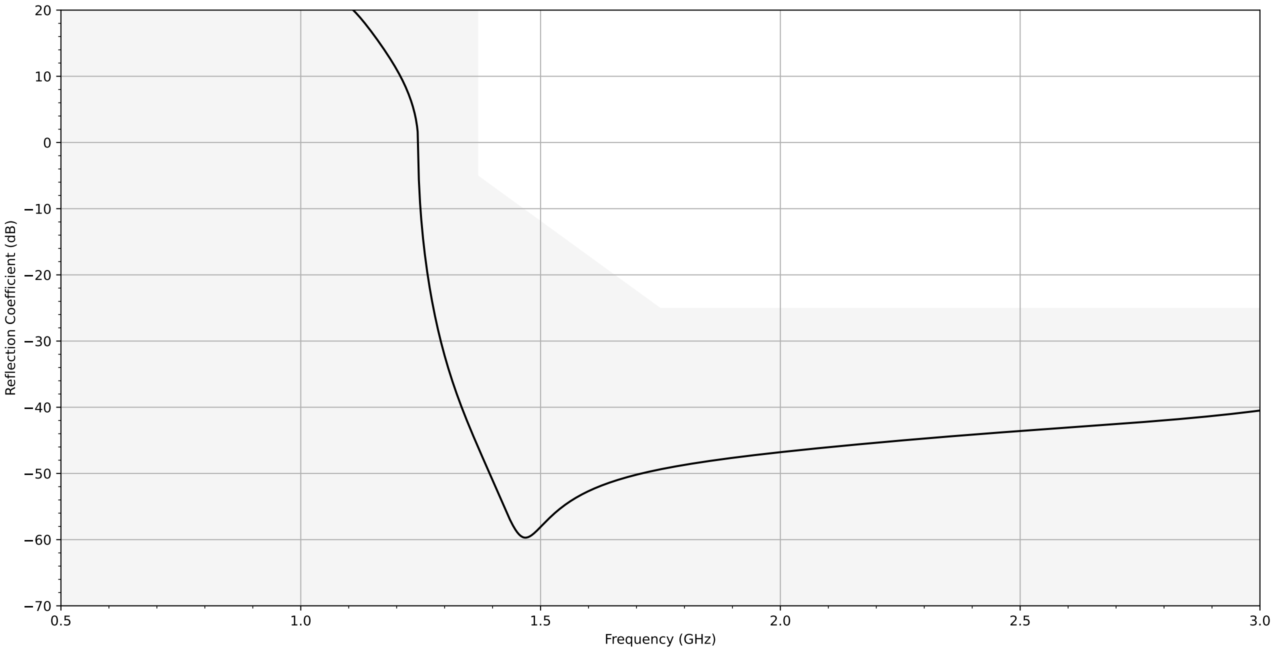

Figure 10: Reflection coefficient for TE, z-axis, x-pol, inhomogen. mesh

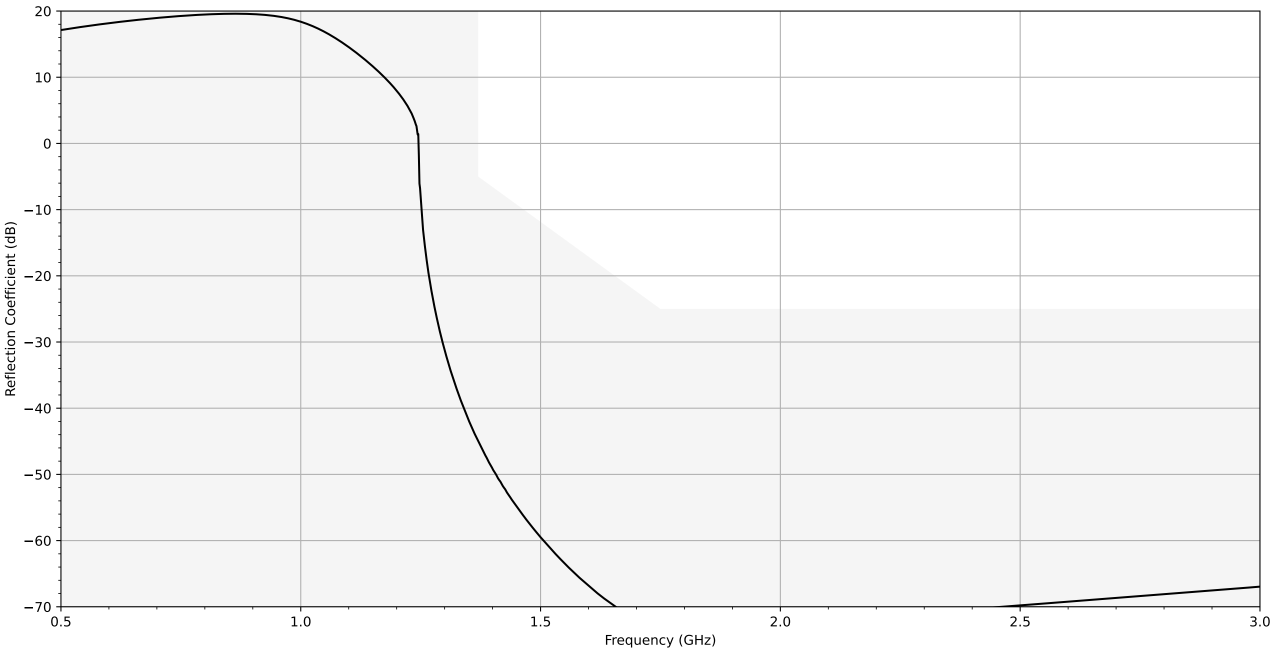

Figure 11: Reflection coefficient for TE, z-axis, y-pol, homogen. mesh

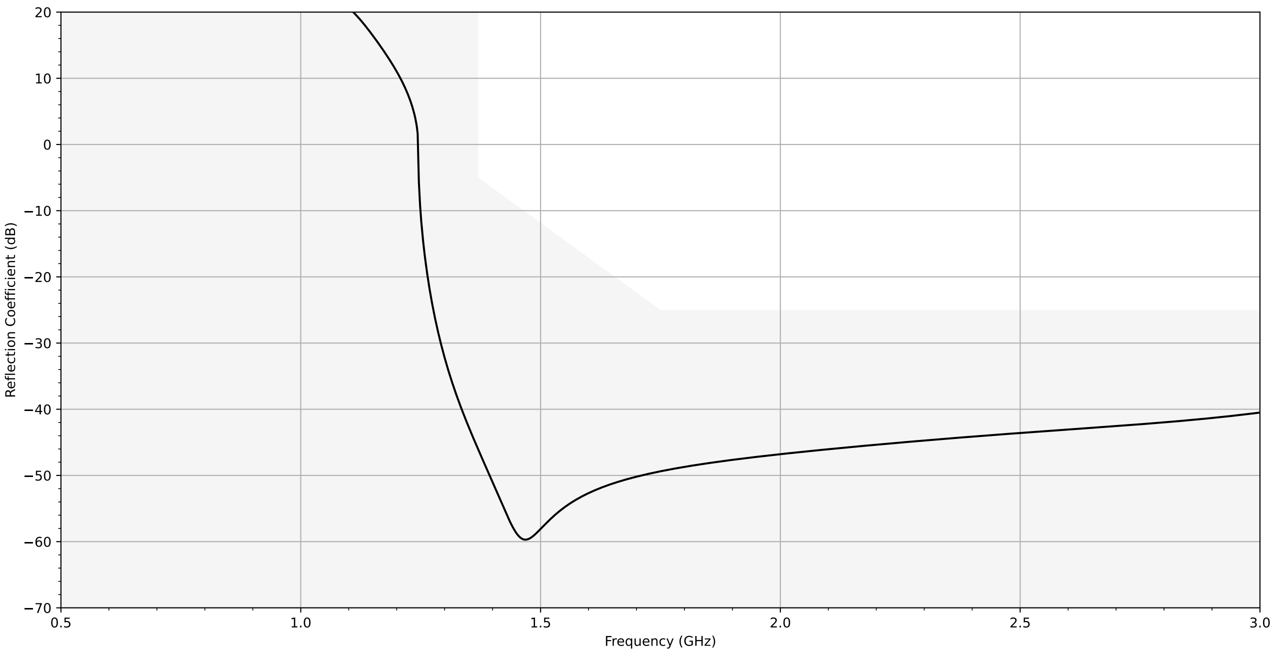

Figure 12: Reflection coefficient for TE, z-axis, y-pol, inhomogen. mesh

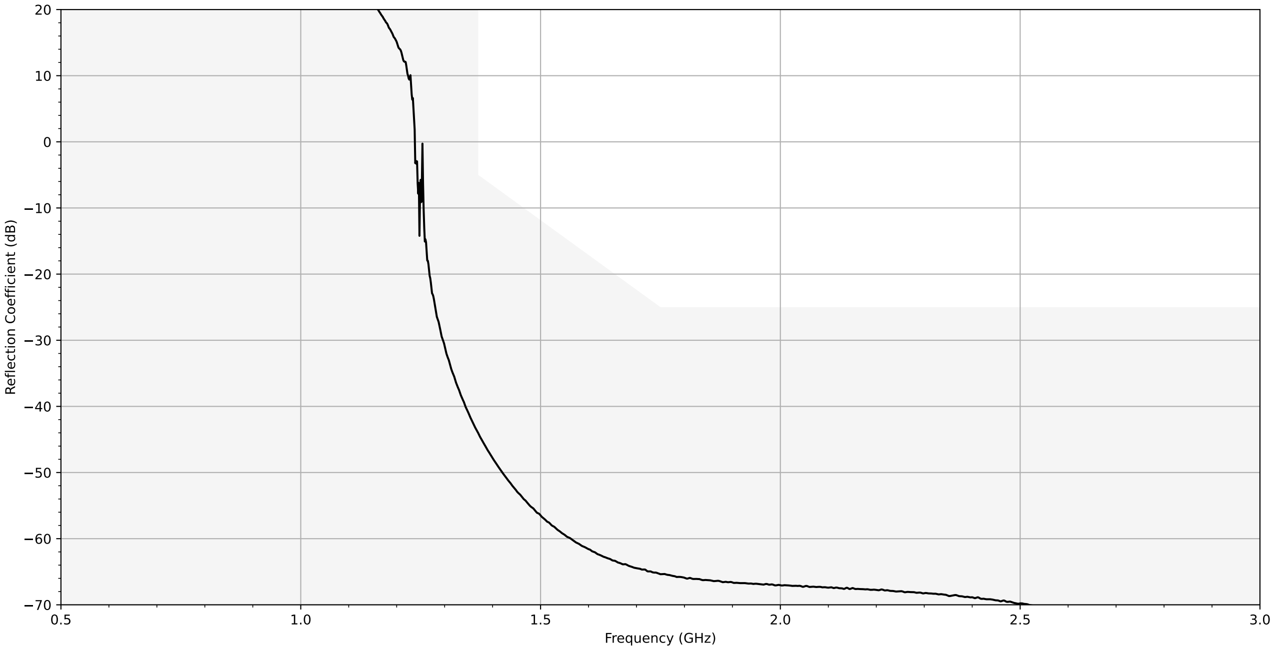

Figure 13: Reflection coefficient for TM, x-axis, y-pol, homogen. mesh

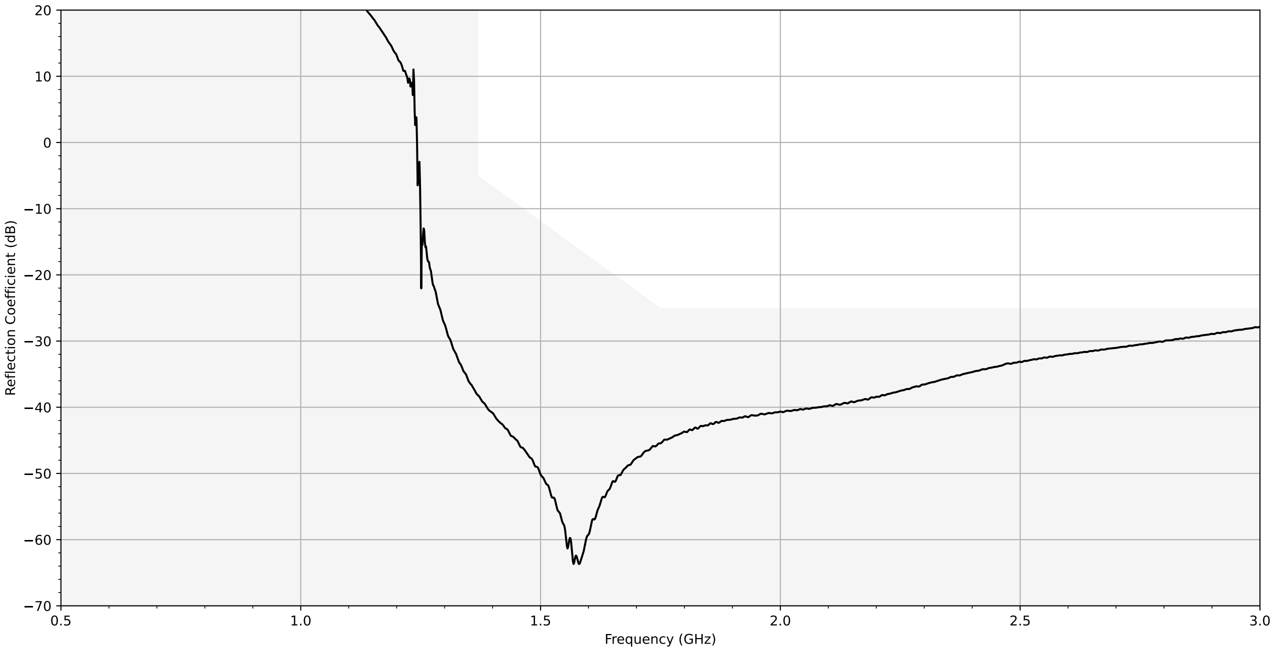

Figure 14: Reflection coefficient for TM, x-axis, y-pol, inhomogen. mesh

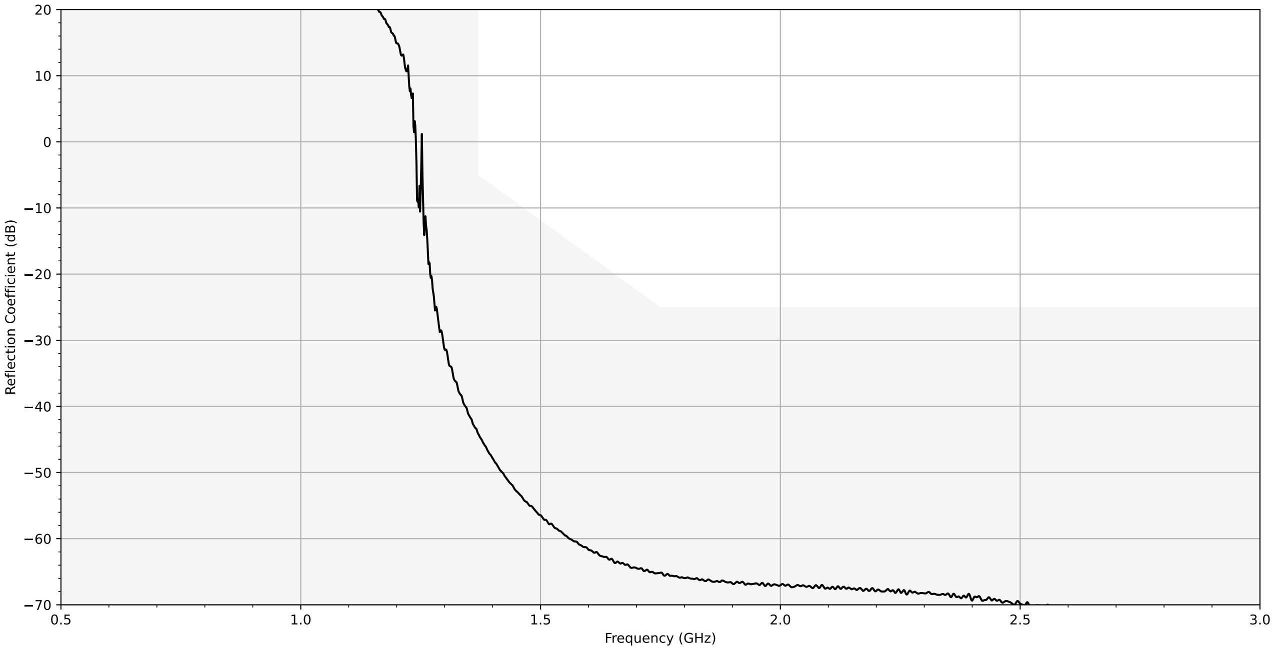

Figure 15: Reflection coefficient for TM, x-axis, z-pol, homogen. mesh

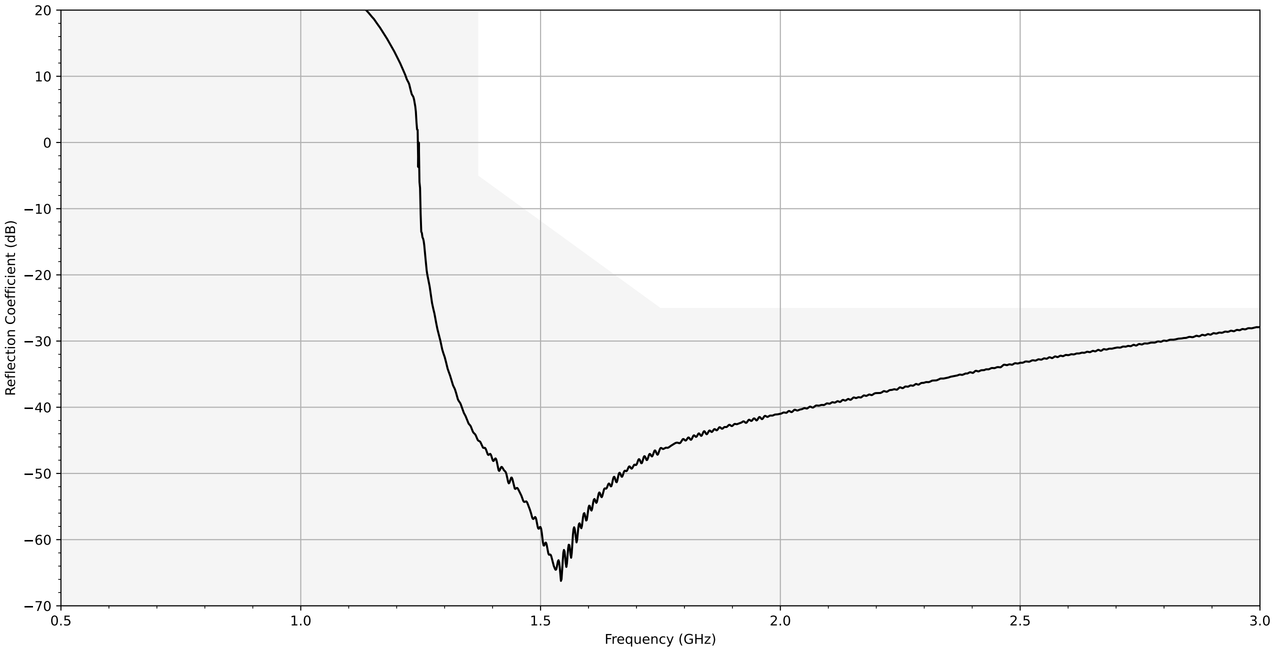

Figure 16: Reflection coefficient for TM, x-axis, z-pol, inhomogen. mesh

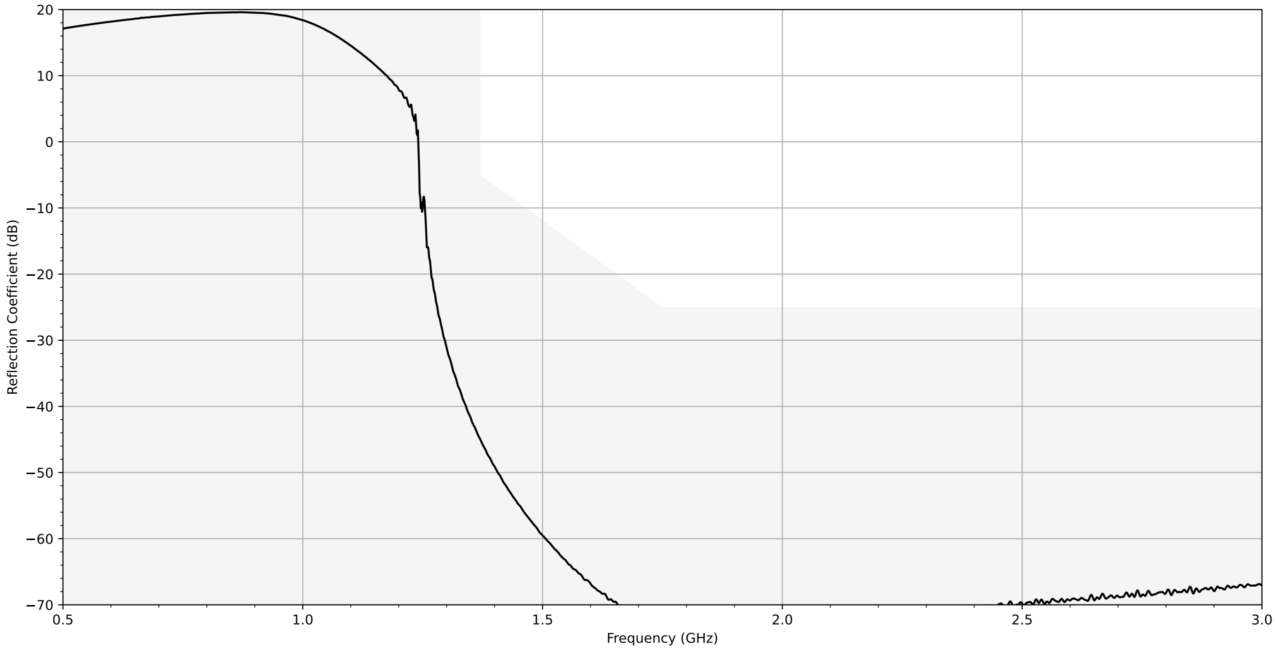

Figure 17: Reflection coefficient for TM, y-axis, x-pol, homogen. mesh

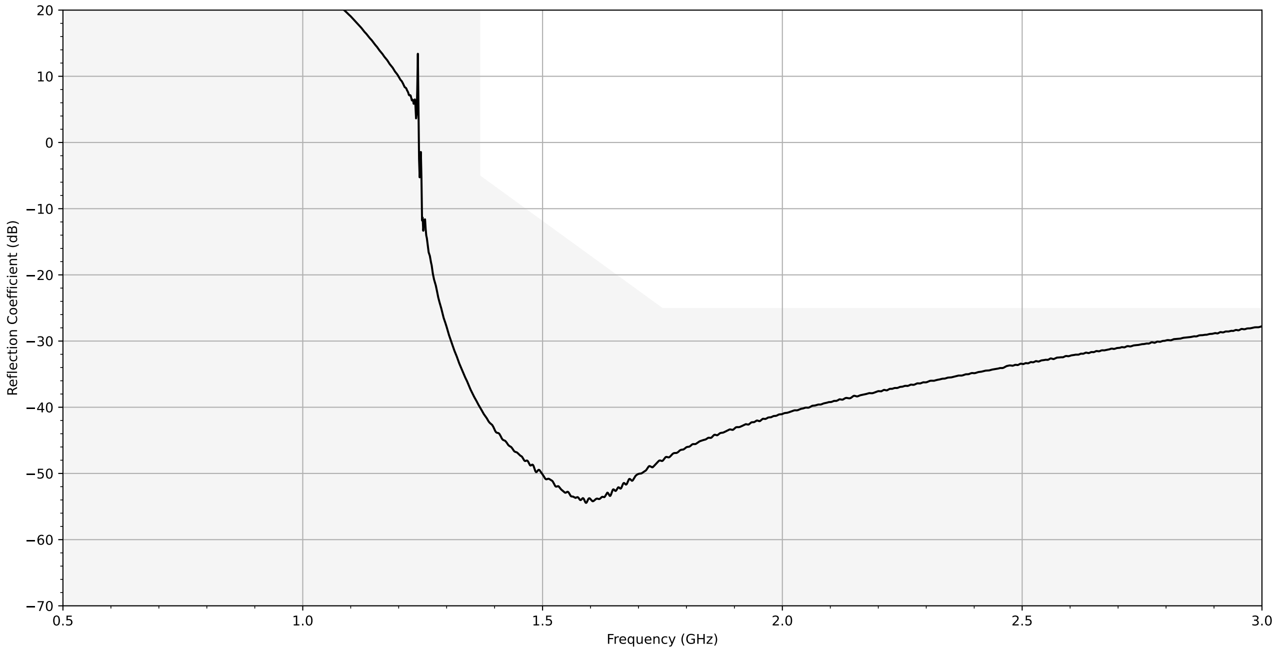

Figure 18: Reflection coefficient for TM, y-axis, x-pol, inhomogen. mesh

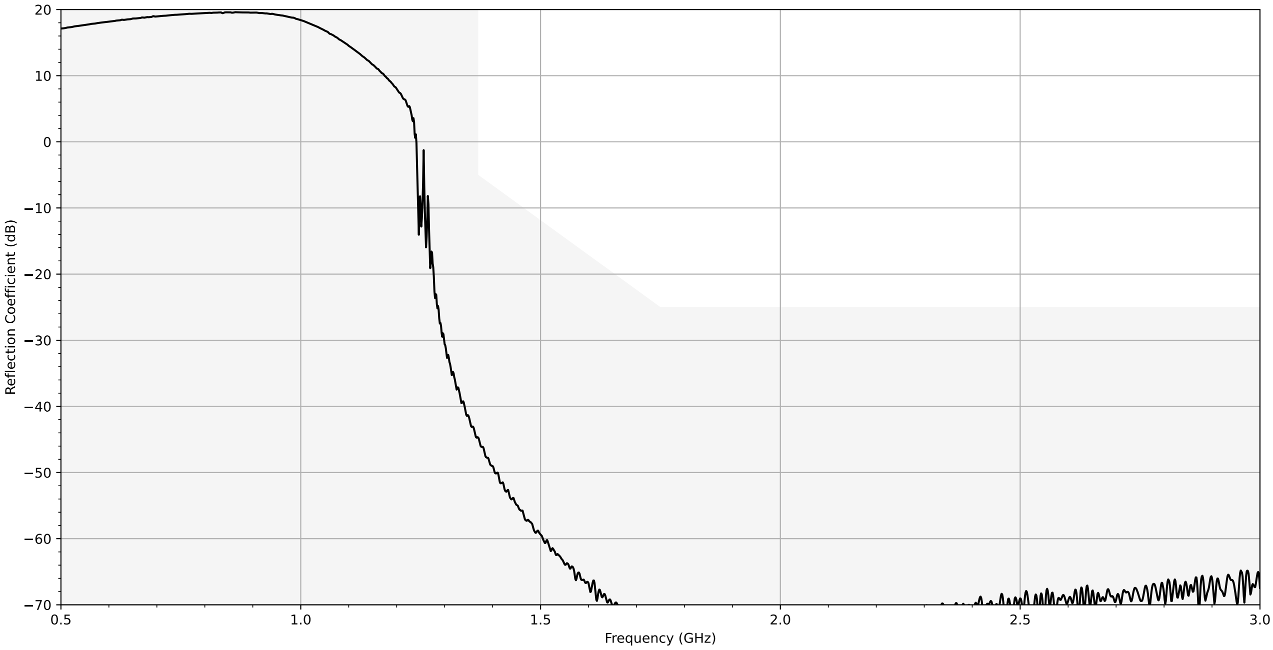

Figure 19: Reflection coefficient for TM, y-axis, z-pol, homogen. mesh

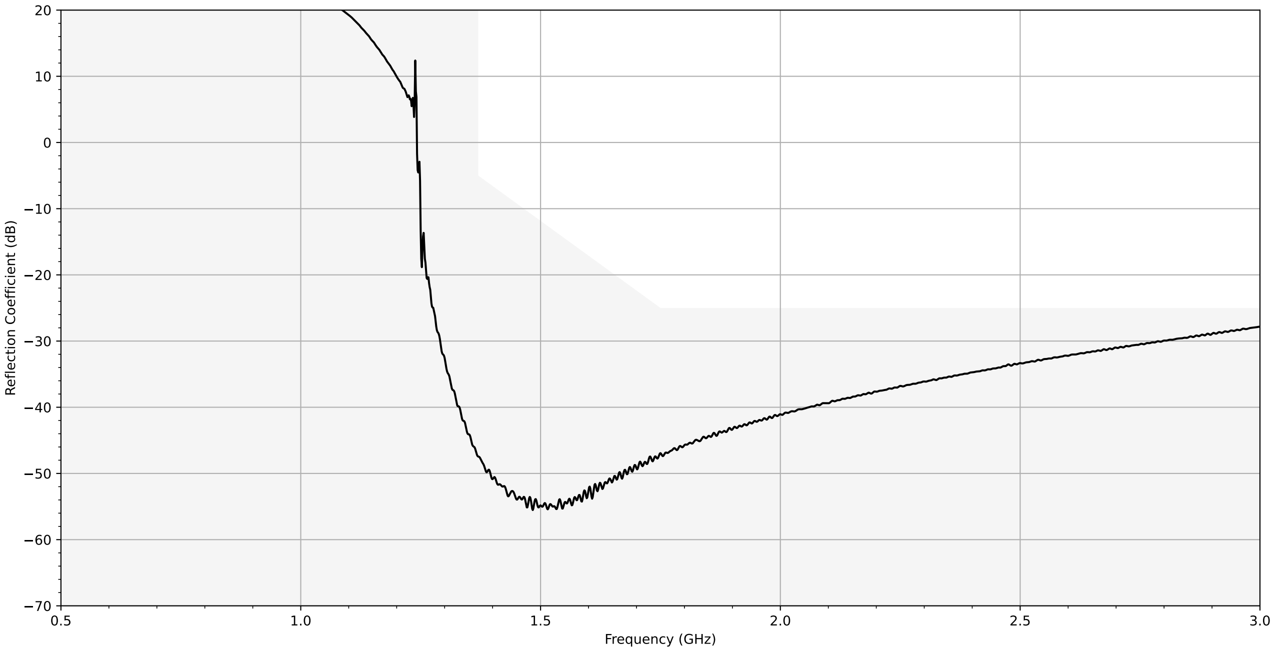

Figure 20: Reflection coefficient for TM, y-axis, z-pol, inhomogen. mesh

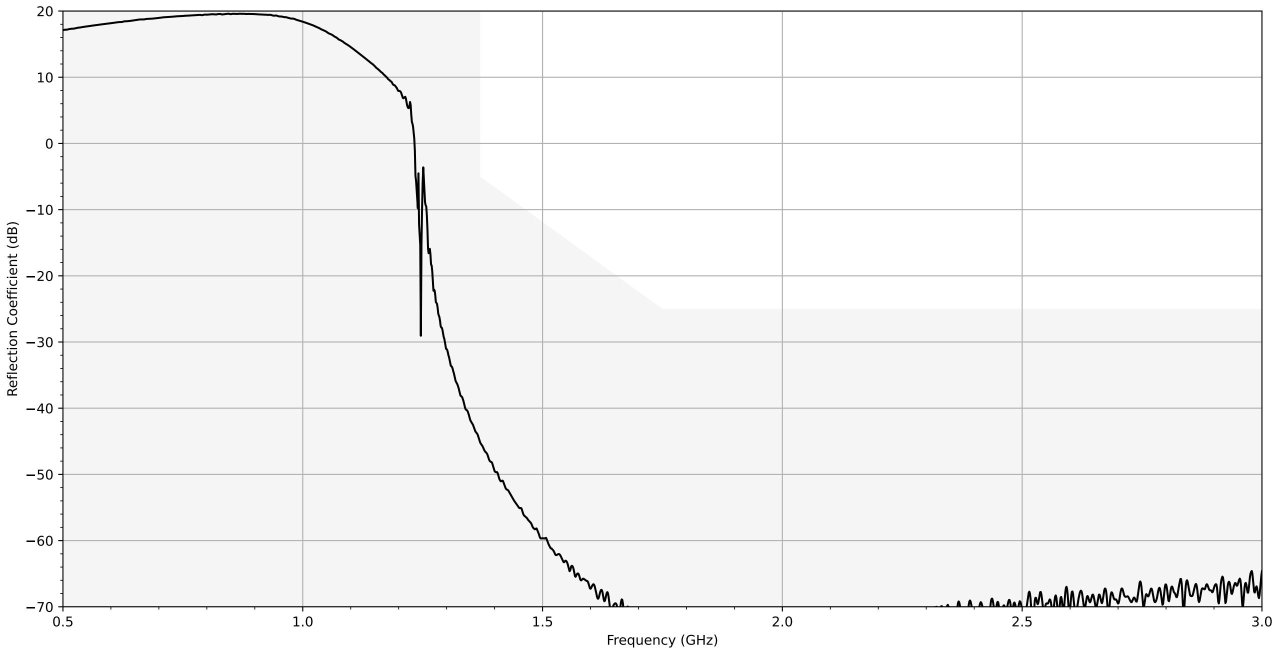

Figure 21: Reflection coefficient for TM, z-axis, x-pol, homogen. mesh

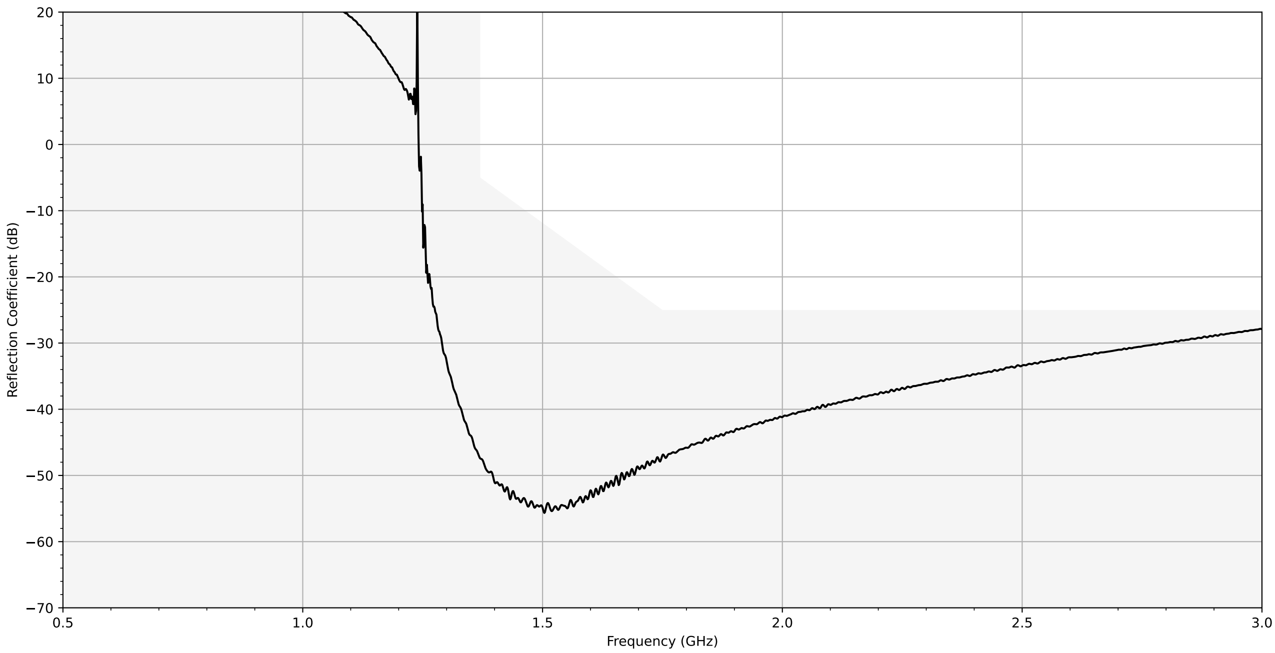

Figure 22: Reflection coefficient for TM, z-axis, x-pol, inhomogen. mesh

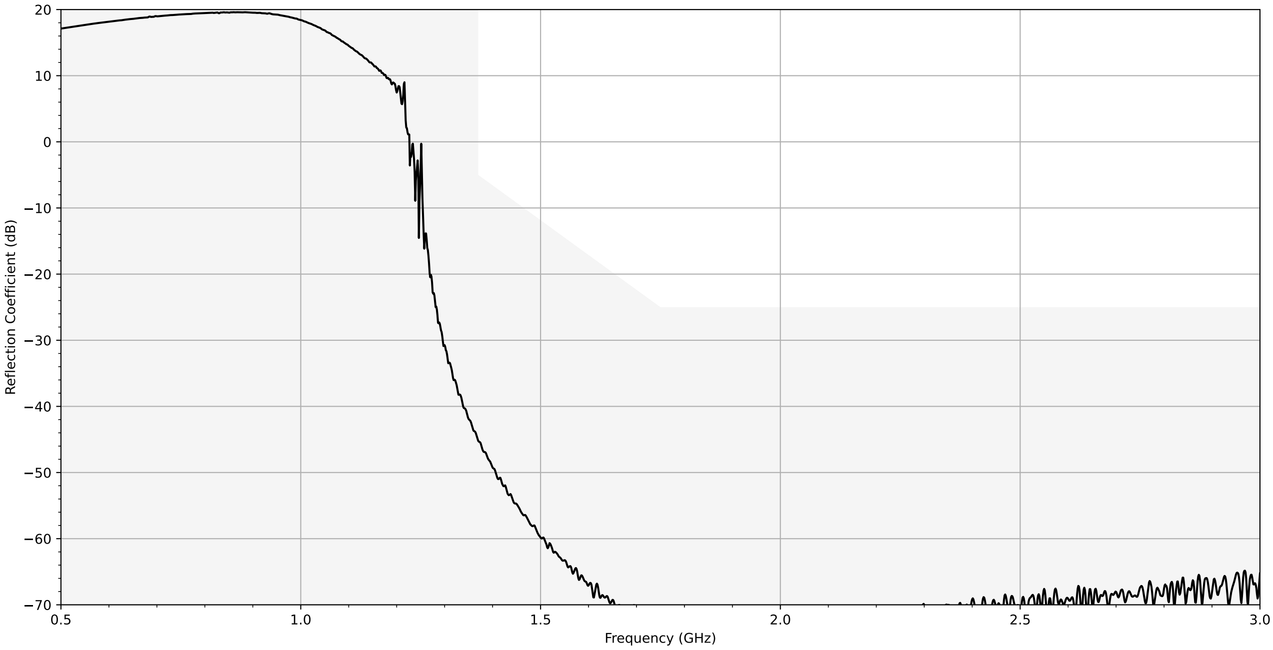

Figure 23: Reflection coefficient for TM, z-axis, y-pol, homogen. mesh

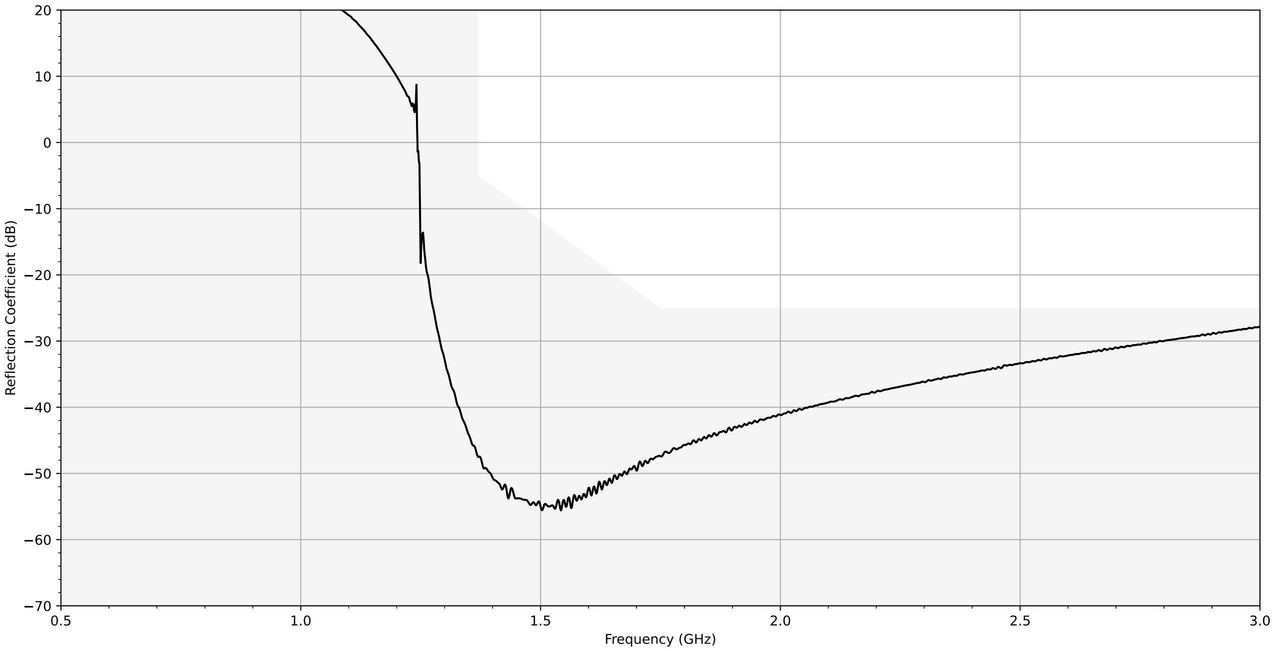

Figure 24: Reflection coefficient for TM, z-axis, y-pol, inhomogen. mesh

2.3.2 Performance of the ABCs in corners of computational domain

The simulation model has been set up as defined in section 8.2.3.2 of IEC/IEEE 62704-1. This section shows the power reflection coefficient in the range of 0.5 to 3 GHz in the permissible range (grey).

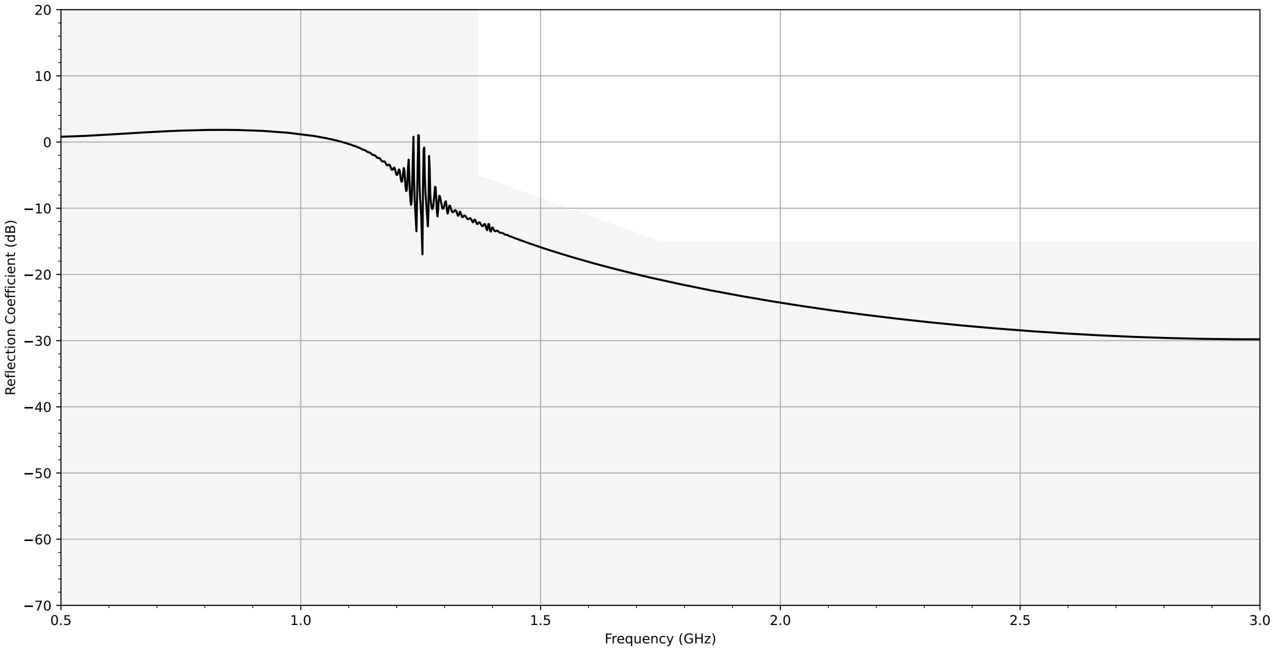

Figure 25: Reflection coefficient for TE case

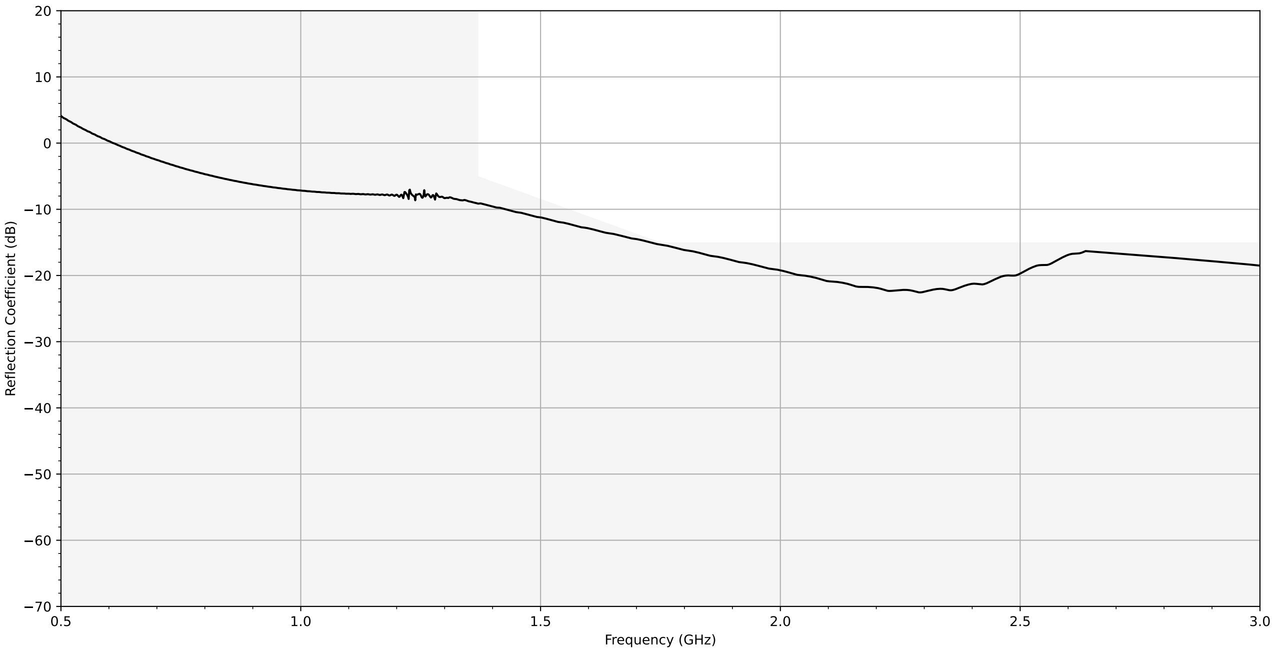

Figure 26: Reflection coefficient for TM case

2.4 SAR Averaging

The SAR averaging compliance evaluation procedure requires to evaluate the averaged SAR in a canonical structure known as the SAR Star as defined in section 8.2.4 of IEC/IEEE 62704-1. The maximum deviation from reference has to be less than 10% and the flagging difference has to be 0 in all cases. For all test cases, EMPIRE XPU achieves compliant results when comparing with reference results published on the IEC/IEEE server. A detailed comparison for the different SAR Star test cases is show below.

2.4.1 SAR Star uniform mesh with 1g averaging

Minimum 1g averaged SAR:	3.53405e-07
Maximum 1g averaged SAR:	0.000164742
Maximum deviation from reference:	4 %
Average deviation from reference:	0.0779588 %
Flagging difference:	0 cells
Orientation difference:	0 cells

DIFFERENCE >	0.01 % :	1472511 cells ,	98.29 % of all cells ,	diff. flagged	0 cells ,	diff. oriented	0 cells.
DIFFERENCE >	0.02 % :	1438407 cells ,	96.01 % of all cells ,	diff. flagged	0 cells ,	diff. oriented	0 cells.
DIFFERENCE >	0.05 % :	1172341 cells ,	78.25 % of all cells ,	diff. flagged	0 cells ,	diff. oriented	0 cells.
DIFFERENCE >	0.10 % :	283687 cells ,	18.94 % of all cells ,	diff. flagged	0 cells ,	diff. oriented	0 cells.
DIFFERENCE >	0.20 % :	42 cells ,	0.00 % of all cells ,	diff. flagged	0 cells ,	diff. oriented	0 cells.
DIFFERENCE >	0.50 % :	4 cells ,	0.00 % of all cells ,	diff. flagged	0 cells ,	diff. oriented	0 cells.
DIFFERENCE >	1.00 % :	1 cells ,	0.00 % of all cells ,	diff. flagged	0 cells ,	diff. oriented	0 cells.
DIFFERENCE >	2.00 % :	1 cells ,	0.00 % of all cells ,	diff. flagged	0 cells ,	diff. oriented	0 cells.
DIFFERENCE >	3.00 % :	1 cells ,	0.00 % of all cells ,	diff. flagged	0 cells ,	diff. oriented	0 cells.
DIFFERENCE >	4.00 % :	1 cells ,	0.00 % of all cells ,	diff. flagged	0 cells ,	diff. oriented	0 cells.
DIFFERENCE >	5.00 % :	0 cells ,	0.00 % of all cells ,	diff. flagged	0 cells ,	diff. oriented	0 cells.

2.4.2 SAR Star uniform mesh with 10g averaging

Minimum 1g averaged SAR:	1.22788e-06
Maximum 1g averaged SAR:	6.91065e-05
Maximum deviation from reference:	0.128501 %
Average deviation from reference:	0.0728294 %
Flagging difference:	0 cells
Orientation difference:	6 cells

DIFFERENCE >	0.01 % :	1490956 cells ,	99.52 % of all cells ,	diff. flagged	0 cells ,	diff. oriented	6 cells.
DIFFERENCE >	0.02 % :	1483384 cells ,	99.01 % of all cells ,	diff. flagged	0 cells ,	diff. oriented	6 cells.
DIFFERENCE >	0.05 % :	1198354 cells ,	79.99 % of all cells ,	diff. flagged	0 cells ,	diff. oriented	6 cells.
DIFFERENCE >	0.10 % :	134190 cells ,	8.96 % of all cells ,	diff. flagged	0 cells ,	diff. oriented	2 cells.
DIFFERENCE >	0.20 % :	0 cells ,	0.00 % of all cells ,	diff. flagged	0 cells ,	diff. oriented	0 cells.

2.4.3 SAR Star graded mesh with 1g averaging

Minimum 1g averaged SAR:	4.36592e-07
Maximum 1g averaged SAR:	0.000148707
Maximum deviation from reference:	0.73141 %
Average deviation from reference:	0.194396 %
Flagging difference:	0 cells
Orientation difference:	1 cells

DIFFERENCE > 0.01 % : 72848 cells , 99.46 % of all cells , diff. flagged 0 cells , diff. oriented 1 cells .
DIFFERENCE > 0.02 % : 72378 cells , 98.81 % of all cells , diff. flagged 0 cells , diff. oriented 1 cells .
DIFFERENCE > 0.05 % : 70460 cells , 96.20 % of all cells , diff. flagged 0 cells , diff. oriented 1 cells .
DIFFERENCE > 0.10 % : 63376 cells , 86.52 % of all cells , diff. flagged 0 cells , diff. oriented 1 cells .
DIFFERENCE > 0.20 % : 20098 cells , 27.44 % of all cells , diff. flagged 0 cells , diff. oriented 0 cells .
DIFFERENCE > 0.50 % : 1803 cells , 2.46 % of all cells , diff. flagged 0 cells , diff. oriented 0 cells .
DIFFERENCE > 1.00 % : 0 cells , 0.00 % of all cells , diff. flagged 0 cells , diff. oriented 0 cells .

2.4.4 SAR Star graded mesh with 10g averaging

Minimum 1g averaged SAR:	1.36945e-06
Maximum 1g averaged SAR:	6.8689e-05
Maximum deviation from reference:	0.621056 %
Average deviation from reference:	0.18621 %
Flagging difference:	0 cells
Orientation difference:	2 cells

DIFFERENCE > 0.01 % : 73247 cells , 100.00 % of all cells , diff. flagged 0 cells , diff. oriented 2 cells .
DIFFERENCE > 0.02 % : 73186 cells , 99.92 % of all cells , diff. flagged 0 cells , diff. oriented 2 cells .
DIFFERENCE > 0.05 % : 72535 cells , 99.03 % of all cells , diff. flagged 0 cells , diff. oriented 2 cells .
DIFFERENCE > 0.10 % : 67770 cells , 92.52 % of all cells , diff. flagged 0 cells , diff. oriented 2 cells .
DIFFERENCE > 0.20 % : 15985 cells , 21.82 % of all cells , diff. flagged 0 cells , diff. oriented 1 cells .
DIFFERENCE > 0.50 % : 916 cells , 1.25 % of all cells , diff. flagged 0 cells , diff. oriented 0 cells .
DIFFERENCE > 1.00 % : 0 cells , 0.00 % of all cells , diff. flagged 0 cells , diff. oriented 0 cells .

3 Canonical Benchmarks

3.1 Generic dipole

The simulation model has been set up as defined in section 8.3.1 of IEC/IEEE 62704-1. This section shows the deviation of the Impedance and power budget.

Dipole Evaluation			
Quantity	**Simulation result (Homogeneous mesh)**	**Simulation result (Inhomogeneous mesh)**	**Tolerance**
Re{Z} at 1 GHz	116.204 Ω	130.166 Ω	$40\,\Omega <$ Re$\{Z\} < 140\,\Omega$
Im{Z} at 1 GHz	42.301 Ω	62.7 Ω	$30\,\Omega <$ Im$\{Z\} < 130\,\Omega$
Frequency for Im{Z} = 0	912.0 MHz	880.0 MHz	850 MHz $< f < 950$ MHz
Power Budget at 0.5 GHz	0.138 %	0.3 %	< 5%
Power Budget at 1.0 GHz	0.022 %	0.164 %	< 5%
Power Budget at 1.50 GHz	0.006 %	0.333 %	< 5%
NOTE 1: The tolerances are the deviations which can be expected from a correctly implemented code which has passed the tests defined in Section 8.2. Larger deviations may indicate errors in the modeling or post-processing environment of the code under evaluation.			

Table 26: Results of the dipole evaluation.

Microstrip Evaluation			
Quantity	**Reference**	**Simulation**	**Tolerance**
Re{Z}	50 Ω	52.19 Ω	$45\,\Omega <$ Re$\{Z\} < 55\,\Omega$
Im{Z}	0	0.02 Ω	$-2\,\Omega <$ Im$\{Z\} < 2\,\Omega$
Reflection coefficient	$-\infty$	-33.08	< -20 dB

Table 27: Results of the microstrip evaluation.

3.2 SAR calculation SAM phantom / generic phone

The simulation model has been set up as defined in section 8.3.3 of IEC/IEEE 62704-1. This section shows the deviation of the peak spatial average SAR values.

1 g and 10 g psSAR for the SAM Phantom exposed to the Generic Phone								
	835 MHz "touch"		**835 MHz "tilted"**		**1900 MHz "touch"**		**1900 MHz "tilted"**	
	Reference	Simulation	Reference	Simulation	Reference	Simulation	Reference	Simulation
1 g psSAR [W/kg]	7.5	7.92	4.9	4.62	8.3	9.93	12.0	12.35
10 g psSAR [W/kg]	5.3	5.78	3.4	3.59	4.8	4.44	6.8	6.11
NOTE: The tolerance of $\pm$50 % is approximately twice the largest standard deviations of the psSAR of the SAM phantom reported in [B2] of IEC/IEEE 62704-1. A larger tolerance is permitted here because of the modifications of the SAR averaging algorithm described in Section 6.2.2 of IEC/IEEE 62704-1								

Table 28: 1 g and 10 g psSAR for the SAM phantom exposed to the generic phone for 1 W accepted antenna power

3.3 System Performance Check

The simulation model has been set up as defined in section 8.3.4 of IEC/IEEE 62704-1. This section shows the deviation of the peak spatial average SAR values and impedance and reports details on domain, mesh steps and power budget.

psSAR and Feedpoint Impedance								
f [MHz]	**1 g psSAR [W/kg]**		**10 g psSAR [W/kg]**		**Re{Z} [Ω]**		**Im{Z} [Ω]**	
	Reference	Simulation	Reference	Simulation	Reference	Simulation	Reference	Simulation
900	11	10.85	7.07	6.95	49.9	50.83	2.3	2.91
3000	65.4	64.97	25.3	26.3	53.4	57.12	-4.0	-4.98
NOTE: The deviation of the peak spatial-average SAR and the real part of the feed-point impedance from the values reported in The simulation model has been set up as defined in section 8.3.4 of IEC/IEEE 62704-1. This section shows the deviation of the peak spatial average SAR values and impedance and reports details on domain, mesh steps and power budget. shall not be larger than $\pm$10 %. The imaginary part of the feed-point impedance shall be within $\pm$ j5 Ω								

Table 29: psSAR normalized to 1 W forward power and feedpoint impedance

Simulation details		
Frequency	**900 MHz**	**3000 MHz**
Overall dimension of computational domain	435mm $\times$ 375mm $\times$ 342 mm	260mm $\times$ 200 mm $\times$ 250 mm
Minimum step in free space	0.25 mm	0.25 mm
Maximum step in free space	10.4 mm	5.14 mm
Minimum step in tissue	0.25 mm	0.25 mm
Maximum step in tissue	1.55 mm	0.80 mm
Dissipated Power (SAR-log)	0.86 W	0.58 W
Radiated Power (FF-log)	0.13 W	0.41 W

Table 30: Dissipated and Radiated Power normalized to 1W forward power.

4 Report History

Revision History				
Version	**Description of Revision**	**Date**	**Revised Page**	**Revised By**
	Initial Release	04.07.2024	-	-